Original Article

Nonlinear dynamic response and vibration of functionally graded nanocomposite cylindrical panel reinforced by carbon nanotubes in thermal environment

Nguyen Dinh Khoa[1], Vu Minh Anh[1,2]
and Nguyen Dinh Duc[1,2,3] (iD)

Abstract

This paper investigated the nonlinear dynamic response and vibration of functionally graded carbon nanotubes-reinforced composite cylindrical panels with the support elastic foundations subjected to mechanical, thermal, and damping loads based on Reddy's higher order shear deformation shell theory. The cylindrical panel is reinforced by single-walled carbon nanotubes which are graded through the panel thickness according to the different linear functions. The effective material properties of the panel are assumed to depend on temperature and estimated through the rule of mixture. The nonlinear dynamic response and natural frequency for functionally graded carbon nanotubes-reinforced composite cylindrical panel are determined by applying the Galerkin method and fourth-order Runge–Kutta method. In numerical results, the effects of geometrical parameters, temperature increment, nanotube volume fraction,

[1]Advanced Materials and Structures Laboratory, VNU-Hanoi, University of Engineering and Technology, Cau Giay, Hanoi, Vietnam
[2]InfrastructureEngineering Program, VNU-Hanoi, Vietnam-Japan University, TuLiem, Hanoi, Vietnam
[3]National Research Laboratory, Department of Civil and Environmental Engineering, Sejong University, Gwangjin-gu, Seoul, Korea

Corresponding author:
Nguyen Dinh Duc, Vietnam National University, 144 Xuan Thuy, Cau Giay, Hanoi, Vietnam.
Email: ducnd@vnu.edu.vn

elastic foundations, and types of carbon nanotubes distributions on the nonlinear vibration of functionally graded carbon nanotubes-reinforced composite cylindrical panel are studied and discussed in detail. The present theory and approach are validated by comparing with those in the literature.

Keywords
Nonlinear dynamic and vibration, functionally graded carbon nanotubes-reinforced composite cylindrical panel, Reddy's higher order shear deformation shell theory, elastic foundations, thermal environment

Introduction

Future applications require materials that are capable of performing well in a variety of environmental conditions, in particular, mechanical, thermal, and chemical properties. Besides, these materials are available in reasonable prices. Functionally graded carbon nanotubes-reinforced composites (FG-CNTRCs) are expected to be a new generation of material that has potential applications in various fields of science and technology such as defense, aerospace, energy, chemical, automotive, and petrochemical industries. They can be gas absorbers, samples or actuators, support catalysts, oil probes, chemical sensors, and nano-reactors. Therefore, FG-CNTRCs are being received considerable attention of researchers and engineering communities for mechanical behaviors. Thermal postbuckling analysis for nanocomposite cylindrical shells reinforced by single-walled carbon nanotubes (SWCNTs) subjected to a uniform temperature rise has been investigated by Shen [1]. Griebel and Hamaekers [2] examined the elastic moduli of polymer–carbon nanotube composites by molecular dynamics simulations of a SWCNT embedded in polyethylene. Zhang and Liew [3] studied viscous fluid-particle mixture induced vibration and instability of FG-CNTRC cylindrical shells integrated with piezoelectric layers. The free vibration characteristics of composite plates reinforced with single-walled carbon nanotubes has been presented by Mirzaei and Kiani [4]. Wave propagation of embedded viscoelastic FG-CNT-reinforced sandwich plates integrated with sensor and actuator based on refined zigzag theory carried out by Kolahchi et al. [5]. Zhang et al. [6] studied a first known investigation on the geometrically nonlinear large deformation behavior of triangular FG-CNTRC plates under transversely distributed loads. Shen and Xiang [7] investigated nonlinear vibration of nanotube-reinforced composite cylindrical panels resting on elastic foundations in thermal environments. Shen and Xiang [8] introduced investigations on the nonlinear bending analysis panels resting on elastic foundations in thermal environments; Kolahchi et al. [9] investigated dynamic stability analysis of temperature-dependent functionally graded CNT-reinforced visco-plates resting on orthotropic elastomeric medium. The linear thermal buckling of a composite conical shell made from a polymeric matrix and

reinforced with carbon nanotube of CNTRC cylindrical fibers has been solved by Mirzaei and Kiani [10]. Mirzaei and Kiani [11] investigated thermal buckling of temperature-dependent FG-CNTRC conical shells. Furthermore, postbuckling of nanotube-reinforced composite cylindrical shells in thermal environments is introduced by Shen [12]. Shen [13] investigated thermal buckling and postbuckling behavior of FG-CNTRC cylindrical shells. The postbuckling analysis of FG-CNTRC plates resting on Pasternak foundations has been presented by Bidgoli et al. [14]. Shen [15] used SWCNTs with the five types of the configurations of carbon nanotubes-reinforced composites in cylindrical panel, FG-V, FG-A, FG-O, FG-X, and UD, to investigate the nonlinear bending of FG-CNTRC plates in thermal environments. Han and Elliott [16] have used molecular dynamic simulations to investigate the effect of volume fraction of single-walled carbon nanotubes on the mechanical of nanocomposites. They indicated that Young's modulus clearly increases when the CNT volume fraction increase.

Recently, many researchers focused on the vibration and dynamic response problem of composite structures because of the optimal purposes and structural safety. Seismic response of functionally graded-carbon nanotubes-reinforced submerged viscoelastic cylindrical shell in hygrothermal environment was studied by Hosseini and Kolahchi [17]. The dynamic stability analysis of moderately thick cylindrical panels made from functionally graded material (FGM) by employing finite strip formulations based on a Reddy-type third-order shear deformation theory has been solved by Ovesy and Fazilati [18]. Viola et al. [19] solved static analysis of functionally graded conical shells and panels using the generalized unconstrained third order theory coupled with the stress recovery. The nonlinear dynamic response and vibration of nanotubes-reinforced composite (FG-CNTRC) shear deformable plates with temperature dependence material properties and surrounded on elastic foundations were considered by Thanh et al. [20]. Ou et al. [21] researches nonlinear dynamic response analysis of cylindrical composite stiffened laminates based on the weak form quadrature element method. Duc and Quan [22] conducted nonlinear response of imperfect eccentrically stiffened FGM cylindrical panels on elastic foundation subjected to mechanical loads. Furthermore, nonlinear mechanical, thermal, and thermo-mechanical postbuckling of imperfect eccentrically stiffened thin FGM cylindrical panels on elastic foundations has been presented by Duc et al. [23]. Thu and Duc [24] studied nonlinear stability analysis of imperfect three-phase sandwich laminated polymer nanocomposite panels resting on elastic foundations in thermal environments. Shen and Wang [25] investigated nonlinear bending of FGM cylindrical panels resting on elastic foundations in thermal environments. Kiani et al. [26] focused on dynamic analysis and active control of smart doubly curved FGM panels. Nonlinear dynamic response and vibration of nanocomposite multilayer organic solar cell were developed by Duc et al. [27].

Furthermore, composite structures are usually subjected to high temperature. The geometrical parameters of structures are deformed and the material properties of structures are changed due to the presence of temperature. Therefore, it is

necessary to take into account the effect of temperature for a better understanding of the mechanical behavior composite plates and shells. Cong et al. [28] focused on nonlinear dynamic response of eccentrically stiffened FGM plate using Reddy's higher order shear deformation shell theory (HSDT) in thermal environment. Najafi et al. [29] evaluated nonlinear dynamic response of FGM beams with Winkler–Pasternak foundation subject to noncentral low velocity impact in thermal field. The nonlinear thermal dynamic analysis of eccentrically stiffened S-FGM circular cylindrical shells surrounded on elastic foundations using HSDT in thermal environment focused is considered by Duc [30]. A finite element formulation for thermally induced vibrations of FGM sandwich plates and shell panels are investigated by Panday and Pradyumna [31]. An analytical approach to investigate the nonlinear dynamic response and vibration of imperfect eccentrically stiffened FGM double curved thin shallow shells on elastic foundation using a simple power-law distribution in thermal environment is presented by Duc and Quan [32]. Yang and Shen [33] developed vibration characteristics and transient response of shear-deformable functionally graded plates in thermal environments. Duc et al. [34] researched nonlinear vibration and dynamic response of imperfect eccentrically stiffened shear deformable sandwich plate with FGM in thermal environment. Yang et al. [35] introduced solution thermo-mechanical postbuckling of FGM cylindrical panels with temperature-dependent properties.

Different from publications above, the novelty of this work is studying about the nonlinear dynamic response and vibration of FG-CNTRC cylindrical panel in thermal environment using HSDT. The cylindrical panels are reinforced by SWCNTs which are graded through the panel thickness according to the different linear functions. The volume fraction and type distribution of carbon nanotubes will be considered. The effective material properties of the panel are assumed to depend on temperature and estimated through the rule of mixture. Numerical results for nonlinear dynamic response and natural frequencies of the FG-CNTRC cylindrical panel are determined by applying the Galerkin method and fourth-order Runge–Kutta method.

The modeling of functionally graded carbon nanotubes reinforced

Assumption that this study considers a FG-CNTRC cylindrical panel is placed in coordinate system (x, y, z) and in which (x, y) plane on the middle surface of the panel and z on thickness direction $(-h/2 \leq z \leq h/2)$ as shown in Figure 1. Besides, the panel is supported by elastic foundation with the thickness h, arc length b, axial length a, and radius of curvature R of the panel.

Elastic modules of CNTRCs and FG-CNTRC

In this study, the FG-CNTRC material consists of poly(methyl methacrylate), PMMA, which is strengthened by (7,7) SWCNTs.
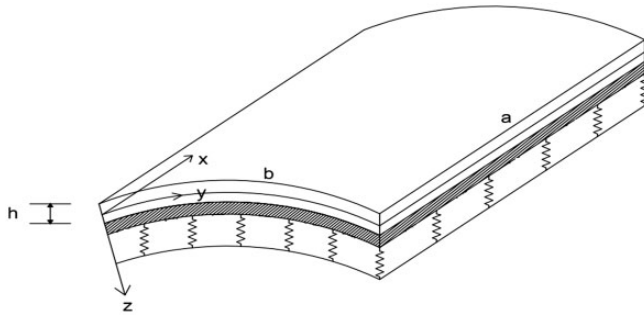
Figure 1. Geometry and coordinate system of functionally graded carbon nanotubes-reinforced composite cylindrical panels on elastic foundations.

According to mixture rule, the effective shear and Young's modulus of the FG-CNTRC material can be given as [1,6–8,10,12]

$$
\begin{aligned}
E_{11} &= \eta_1 V_{CNT} E_{11}^{CNT} + V_m E_m, \\
\frac{\eta_2}{E_{22}} &= \frac{V_{CNT}}{E_{22}^{CNT}} + \frac{V_m}{E_m}, \\
\frac{\eta_3}{G_{12}} &= \frac{V_{CNT}}{G_{12}^{CNT}} + \frac{V_m}{G_m}
\end{aligned}
\tag{1}
$$

where V_m and V_{CNT} are the volume fractions of the matrix and the carbon nanotubes, respectively. $G_{12}^{CNT}, E_{11}^{CNT}, E_{22}^{CNT}$ are shear and Young's modulus of the FG-CNTRCs layer; E_m and G_m are corresponding properties of the matrix and η_i ($i = \overline{1,3}$) are the carbon nanotubes efficiency parameters.

In this study, we consider five types of FG-CNTRC: FG-O, FG-V, FG-X, UD, and FG-A as Figure 2. The distribution of the volume fractions of the matrix and the carbon nanotubes change according to the panel thickness are the linear functions. The volume fractions of the FG-CNTRC take the following forms [4,6,10]

$$
V_{CNT}(z) = \begin{cases}
2V_{VCT}^* \left(2\dfrac{|z|}{h} \right) & (FG-X) \\[2ex]
V_{VCT}^* \left(1 - 2\dfrac{|z|}{h} \right) & (FG-V) \\[2ex]
V_{VCT}^* \left(1 + 2\dfrac{z}{h} \right) & (FG-A) \\[2ex]
2V_{VCT}^* \left(1 - 2\dfrac{|z|}{h} \right) & (FG-O) \\[2ex]
V_{VCT}^* (UD)
\end{cases}
, \quad V_m(z) = 1 - V_{CNT}(z)
\tag{2}
$$

where

$$V^*_{CNT} = \frac{w_{CNT}}{w_{CNT} + (\rho_{CNT}/\rho_m) - (\rho_{CNT}/\rho_m)w_{CNT}} \tag{3}$$

where ρ_m, ρ_{CNT} and w_{CNT} are the densities of matrix and carbon nanotubes, the mass fraction of carbon nanotubes, respectively. The effective Poisson's ratio is function depends on position and temperature change. Moreover, the thermal expansion coefficients in the transverse and longitudinal directions of the FG-CNTRC and is written as [1,6–8, 10,12]

$$\nu_{12} = V^*_{CNT}\nu^{CNT}_{12} + V_m\nu_m \tag{4}$$

where ν^{CNT}_{12} and ν_m are Poisson's ratio of the carbon nanotubes and the matrix, respectively.

$$\alpha_{11} = \frac{V_{CNT}E^{CNT}_{11}\alpha^{CNT}_{11} + V_mE_m\alpha_m}{V_{CNT}E^{CNT}_{11} + V_mE_m},$$
$$\alpha_{22} = (1 + \nu^{CNT}_{12})V_{CNT}\alpha^{CNT}_{22} + (1 + \nu_m)V_m\alpha_m - \nu_{12}\alpha_{11} \tag{5}$$

in which α_m and α^{CNT}_{11}, α^{CNT}_{22} are the thermal expansion coefficients of the matrix and the carbon nanotubes, respectively.

The materials properties of matrix are given as [1,6–8, 10,12]

$$\nu_m = 0.34, \ \alpha_m = 45(1 + 0.0005\Delta T) \times 10^{-6}/\text{K},$$
$$E_m = (3.52 - 0.0034T)\,\text{GPa} \tag{6}$$

with $T = T_0 + \Delta T$, $T_0 = 300\,\text{K}$ (room temperature) and ΔT is the temperature increment.

For the carbon nanotubes, the material properties of (7,7) SWCNTs are highly dependent to temperature. According to Shen and Xiang [8], based on the Poisson's ratio of SWCNTs with conditions are $\nu^{CNT}_{12} = 0.175$ and thickness obtained for $h = 0.067\,\text{m}$. These properties of SWCNTs at five certain temperature levels, i.e., $T = 300, 400, 500, 700, 1000$ are determined. Specifically, thermal expansion coefficient, shear modulus, and Young's modulus of SWCNTs are listed in Table 1.

$\eta_i \ (i = \overline{1,3})$, which are carbon nanotubes efficiency parameters, are introduced in equation (1). These values of $\eta_i \ (i = \overline{1,3})$ are estimated by matching the effective properties of FG-CNTRC material: the shear modulus G_{12} and Young's modulus E_{11} and E_{22}. The carbon nanotubes efficiency parameters utilized in this paper are as given in Table 2 [1,6–8,10,12].
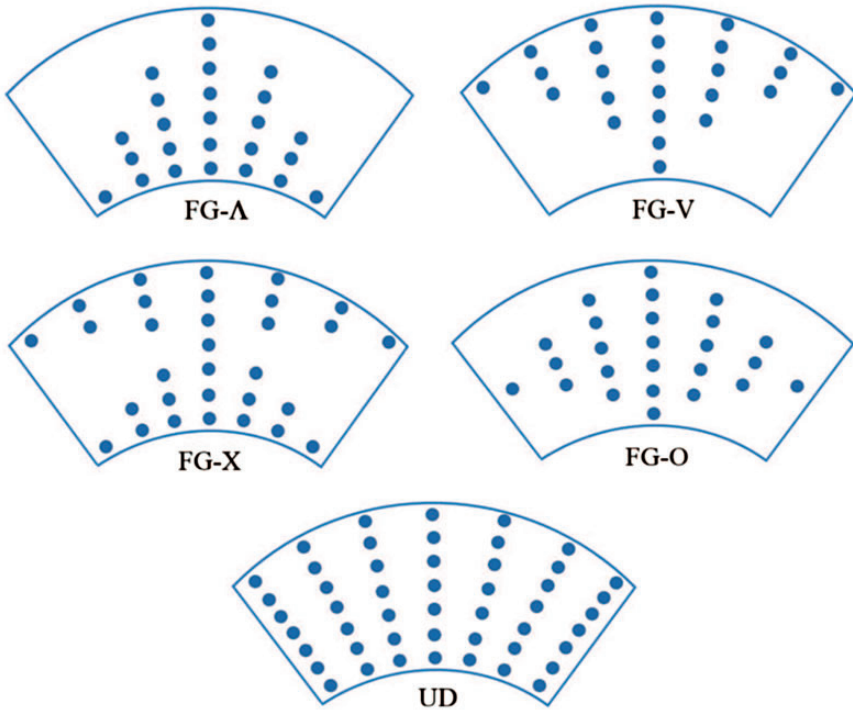
Figure 2. The configurations of five types of functionally graded carbon nanotubes -reinforced composites in cylindrical panel.

Table 1. Temperature-dependent material properties for (7, 7) SWCNTs ($\nu_{12}^{CNT} = 0.175$ and $h = 0.067$ m).

T (K)	E_{11}^{CNT} (TPa)	E_{22}^{CNT} (TPa)	G_{12}^{CNT} (TPa)	α_{11}^{CNT} ($\times 10^{-6}$/K)	α_{22}^{CNT} ($\times 10^{-6}$/K)
300	5.6466	7.0800	1.9445	3.4584	5.1682
400	5.5679	6.9814	1.9703	4.1496	5.0905
500	5.5308	6.9348	1.9643	4.5361	5.0189
700	5.4744	6.8641	1.9644	4.6677	4.8943
1000	5.2814	6.6220	1.9451	4.2800	4.7532

Basic equations

The geometrical compatibility equation for a FG-CNTRC cylindrical panel is written as [37–39]

$$\frac{\partial^2 \varepsilon_x^0}{\partial y^2} + \frac{\partial^2 \varepsilon_y^0}{\partial x^2} - \frac{\partial^2 \gamma_{xy}^0}{\partial x \partial y} = \left(\frac{\partial^2 w}{\partial x \partial y}\right)^2 - \frac{\partial^2 w}{\partial x^2}\frac{\partial^2 w}{\partial y^2} - \frac{1}{R}\frac{\partial^2 w}{\partial x^2} \tag{7}$$

Table 2. The CNT efficiency parameters for (7, 7).

V^*_{CNT}	Rule of mixture		
	η_1	η_2	η_3
0.12	0.137	1.022	0.715
0.17	0.142	1.626	1.138
0.28	0.141	1.585	1.109

where ε^0_x, ε^0_y and γ^0_{xy} are normal strains and the shear strain at the middle surface of the panel, respectively.

The nonlinear equilibrium equation of a FG-CNTRC cylindrical panel on the elastic foundations is written as [37–39]

$$\frac{\partial N_x}{\partial x} + \frac{\partial N_{xy}}{\partial y} = J_0 \frac{\partial^2 u}{\partial t^2} + I_1 \frac{\partial^2 \varphi_x}{\partial t^2} - c_1 J_3 \frac{\partial^3 w}{\partial x \partial t^2} \tag{8a}$$

$$\frac{\partial N_{xy}}{\partial x} + \frac{\partial N_y}{\partial y} = J_0 \frac{\partial^2 v}{\partial t^2} + I_1 \frac{\partial^2 \varphi_y}{\partial t^2} - c_1 J_3 \frac{\partial^3 w}{\partial y \partial t^2} \tag{8b}$$

$$\begin{aligned}
&\frac{\partial Q_x}{\partial x} + \frac{\partial Q_y}{\partial y} - c_2 \left(\frac{\partial R_x}{\partial x} + \frac{\partial R_y}{\partial y} \right) + N_x \frac{\partial^2 w}{\partial x^2} + 2N_{xy} \frac{\partial^2 w}{\partial x \partial y} \\
&+ N_y \frac{\partial^2 w}{\partial y^2} + c_1 \left(\frac{\partial^2 P_x}{\partial x^2} + 2 \frac{\partial^2 P_{xy}}{\partial x \partial y} + \frac{\partial^2 P_y}{\partial y^2} \right) + \frac{N_y}{R} - k_1 w + k_2 \left(\frac{\partial^2 w}{\partial x^2} + \frac{\partial^2 w}{\partial y^2} \right) + q \\
&= J_0 \frac{\partial^2 w}{\partial t^2} + 2\varepsilon J_0 \frac{\partial w}{\partial t} - c_1^2 J_6 \left(\frac{\partial^4 w}{\partial x^2 \partial t^2} + \frac{\partial^4 w}{\partial y^2 \partial t^2} \right) \\
&+ c_1 \left[J_3 \left(\frac{\partial^3 u}{\partial x \partial t^2} + \frac{\partial^3 v}{\partial y \partial t^2} \right) + I_4 \left(\frac{\partial^3 \varphi_1}{\partial x \partial t^2} + \frac{\partial^3 \varphi_2}{\partial y \partial t^2} \right) \right]
\end{aligned} \tag{8c}$$

$$\frac{\partial M_x}{\partial x} + \frac{\partial M_{xy}}{\partial y} - c_1 \left(\frac{\partial P_x}{\partial x} + \frac{\partial P_{xy}}{\partial y} \right) - Q_x + c_2 R_x = I_1 \frac{\partial^2 u}{\partial t^2} + V_2 \frac{\partial^2 \varphi_x}{\partial t^2} - c_1 I_4 \frac{\partial^3 w}{\partial x \partial t^2} \tag{8d}$$

$$\frac{\partial M_{xy}}{\partial x} + \frac{\partial M_y}{\partial y} - c_1 \left(\frac{\partial P_{xy}}{\partial x} + \frac{\partial P_y}{\partial y} \right) - Q_y + c_2 R_y = I_1 \frac{\partial^2 v}{\partial t^2} + V_2 \frac{\partial^2 \varphi_y}{\partial t^2} - c_1 I_4 \frac{\partial^3 w}{\partial y \partial t^2} \tag{8e}$$

where

$$J_i = \int_{-h/2}^{h/2} \rho(z) z^i \mathrm{d}z, \quad (i = 0, 1, 2, 3, 4, 6),$$

$$I_i = J_i - c_1 J_{i+2}, \quad V_2 = J_2 - 2c_1 J_4 + c_1^2 J_6, \quad c_2 = 3c_1,$$

$$\rho(z) = V_{CNT} \rho_{CNT} + V_m \rho_m$$

(9)

and u, v, w are displacement components corresponding to the coordinates (x, y, z); k_1 is Winkler foundation modulus; k_2 is the shear layer foundation stiffness of Pasternak model; ε is the viscous damping coefficient; coefficients $I_i(i = 0 \div 4, 6)$ are given in Appendix 1.

In the middle surface, the normal and shear strains of FG-CNTRC cylindrical panels are defined as

$$\varepsilon_x^0 = \frac{\partial u^0}{\partial x} - \frac{w^0}{R} + \frac{1}{2}\left(\frac{\partial w^0}{\partial x}\right)^2, \quad \varepsilon_y^0 = \frac{\partial v^0}{\partial y} + \frac{1}{2}\left(\frac{\partial w^0}{\partial y}\right)^2$$

$$\gamma_{xy}^0 = \frac{\partial u^0}{\partial y} + \frac{\partial v^0}{\partial x} + \frac{\partial w^0}{\partial x}\frac{\partial w^0}{\partial y}$$

(10)

In which u^0, v^0, w^0 are displacement component of a genetic point on the reference surface.

The relationships between strain and displacements at a distance "z" using HSDT and von Karman nonlinear terms are [36,37]

$$\varepsilon_x = \varepsilon_x^0 - z\frac{\partial^2 w^0}{\partial x^2} + f(z)\frac{\partial \phi_1^0}{\partial x}$$

$$\varepsilon_y = \varepsilon_y^0 - z\frac{\partial^2 w^0}{\partial y^2} + f(z)\frac{\partial \phi_2^0}{\partial y}$$

$$\gamma_{xy} = \gamma_{xx}^0 - 2z\frac{\partial^2 w^0}{\partial x \partial y} + f(z)\frac{\partial \phi_1^0}{\partial y} + f(z)\frac{\partial \phi_2^0}{\partial x}$$

(11)

$$\gamma_{xz} = \frac{\partial u}{\partial z} + \frac{\partial w}{\partial x} = f'(z)\phi_1^0$$

$$\gamma_{yz} = \frac{\partial v}{\partial z} + \frac{\partial w}{\partial y} = f'(z)\phi_2^0$$

with

$$\phi_1^0 = \varphi_x + \frac{\partial w^0}{\partial x}, \quad \phi_2^0 = \varphi_y + \frac{\partial w^0}{\partial y}$$

$$f(z) = z\left[1 - (4/3)(z/h)^2\right]$$

$$f'(z) = \frac{d}{dz}f(z)$$

(12)

where φ_x and φ_y are rotation angles around the x and y axes, respectively.

Hooke's law for a FG-CNTRC cylindrical panel is defined as [7]

$$\begin{bmatrix} \sigma_{xx} \\ \sigma_{yy} \\ \sigma_{xy} \\ \sigma_{xz} \\ \sigma_{yz} \end{bmatrix} = \begin{bmatrix} Q_{11} & Q_{12} & 0 & 0 & 0 \\ Q_{12} & Q_{22} & 0 & 0 & 0 \\ 0 & 0 & Q_{66} & 0 & 0 \\ 0 & 0 & 0 & Q_{44} & 0 \\ 0 & 0 & 0 & 0 & Q_{55} \end{bmatrix} \begin{Bmatrix} \varepsilon_{xx} \\ \varepsilon_{yy} \\ \varepsilon_{xy} \\ \varepsilon_{xz} \\ \varepsilon_{yz} \end{Bmatrix} - \Delta T \begin{Bmatrix} \alpha_{11} \\ \alpha_{22} \\ 0 \\ 0 \\ 0 \end{Bmatrix}$$

(13)

where

$$Q_{11} = \frac{E_{11}}{1 - \nu_{12}\nu_{21}}, \quad Q_{22} = \frac{E_{22}}{1 - \nu_{12}\nu_{21}}, \quad Q_{12} = \frac{\nu_{21}E_{11}}{1 - \nu_{12}\nu_{21}}, \quad Q_{44} = G_{23},$$

$$Q_{55} = G_{13}, \quad Q_{44} = G_{12}$$

(14)

According to Shen [1], we assume that $G_{13} = G_{12}$ and $G_{23} = 1.2G_{12}$

The force and moment resultants of FG-CNTRC cylindrical panel are determined by

$$(N_i, M_i, P_i) = \int_{-h/2}^{h/2} \sigma_i(1, z, z^3)dz, \quad i = x, y, xy,$$

$$(Q_i, K_i) = \int_{-h/2}^{h/2} \sigma_{iz}(1, z^2)dz, \quad i = x, y$$

(15)

Inserting equations (11) and (13) into equations (15), the constitutive relations are obtained as

$$N_x = C_{11}\varepsilon_x^0 + C_{12}\varepsilon_y^0 + C_{13}k_x^1 + C_{14}k_y^1 + C_{15}k_x^3 + C_{16}k_y^3 - \Phi_x^1,$$

$$N_y = C_{12}\varepsilon_x^0 + C_{22}\varepsilon_y^0 + C_{14}k_x^1 + C_{24}k_y^1 + C_{16}k_x^3 + C_{26}k_y^3 - \Phi_y^1,$$

$$N_{xy} = C_{31}\gamma_{xy}^0 + C_{32}k_{xy}^1 + C_{33}k_{xy}^3,$$

$$M_x = C_{13}\varepsilon_x^0 + C_{14}\varepsilon_y^0 + C_{43}k_x^1 + C_{44}k_y^1 + C_{45}k_x^3 + C_{46}k_y^3 - \Phi_x^2,$$

$$M_y = C_{14}\varepsilon_x^0 + C_{24}\varepsilon_y^0 + C_{44}k_x^1 + C_{54}k_y^1 + C_{46}k_x^3 + C_{56}k_y^3 - \Phi_y^2,$$

$$M_{xy} = C_{32}\gamma_{xy}^0 + C_{62}k_{xy}^1 + C_{63}k_{xy}^3,$$

$$P_x = C_{15}\varepsilon_x^0 + C_{16}\varepsilon_y^0 + C_{45}k_x^1 + C_{46}k_y^1 + C_{75}k_x^3 + C_{76}k_y^3 - \Phi_x^3,$$

$$P_y = C_{16}\varepsilon_x^0 + C_{26}\varepsilon_y^0 + C_{46}k_x^1 + C_{56}k_y^1 + C_{76}k_x^3 + C_{86}k_y^3 - \Phi_y^3,$$

$$P_{xy} = C_{33}\gamma_{xy}^0 + C_{63}k_{xy}^1 + C_{93}k_{xy}^3,$$

$$Q_x = G_{11}\gamma_{xz}^0 + G_{12}k_{xz}^2,$$

$$Q_y = G_{21}\gamma_{yz}^0 + G_{22}k_{yz}^2,$$

$$K_x = G_{12}\gamma_{xz}^0 + G_{32}k_{xz}^2,$$

$$K_y = G_{22}\gamma_{yz}^0 + G_{42}k_{yz}^2$$

(16)

and the linear parameters $C_{1j}(j = \overline{1,6}), C_{2j}(j = 2,4,6), C_{3j}(j = \overline{1,3}),$ $C_{4j}(j = \overline{3,6}), C_{5j}(j = 4,6),$ $C_{6j}(j = 2,3), C_{7j}(j = 5,6), C_{i6}(i = 8,9),$ $G_{ij}(i,j = \overline{4,2}),$ $\Phi_{xi}(i = \overline{1,3}), \Phi_{yi}(i = \overline{1,3})$ are given in Appendix 1.

Calculating from equations (12) and equations (16), one can write

$$\varepsilon_x^0 = H_{11}N_x - H_{12}N_y + H_{13}k_x^1 + H_{14}k_y^1 + H_{15}k_x^3 + H_{16}k_y^3 + H_{11}\Phi_x^1 - H_{12}\Phi_y^1,$$

$$\varepsilon_y^0 = -H_{12}N_x + H_{22}N_y + H_{23}k_x^1 + H_{24}k_y^1 + H_{25}k_x^3 + H_{26}k_y^3 - H_{12}\Phi_x^1 + H_{22}\Phi_y^1,$$

$$\gamma_{xy}^0 = \frac{1}{C_{31}}N_{xy} - \frac{C_{32}}{C_{31}}k_{xy}^1 - \frac{C_{33}}{C_{31}}k_{xy}^3$$

(17)

with

$$H_{11} = \frac{C_{22}}{C_{11}C_{22} - C_{12}^2}, \quad H_{12} = \frac{C_{12}}{C_{11}C_{22} - C_{12}^2}, \quad H_{13} = \frac{C_{14}C_{12} - C_{13}C_{22}}{C_{11}C_{22} - C_{12}^2},$$

$$H_{14} = \frac{C_{24}C_{12} - C_{14}C_{22}}{C_{11}C_{22} - C_{12}^2}, \quad H_{15} = \frac{C_{16}C_{12} - C_{15}C_{22}}{C_{11}C_{22} - C_{12}^2}, \quad H_{16} = \frac{C_{26}C_{12} - C_{16}C_{22}}{C_{11}C_{22} - C_{12}^2},$$

$$H_{22} = \frac{C_{11}}{C_{11}C_{22} - C_{12}^2}, \quad H_{23} = \frac{C_{13}C_{12} - C_{14}C_{11}}{C_{11}C_{22} - C_{12}^2}, \quad H_{24} = \frac{C_{14}C_{12} - C_{24}C_{11}}{C_{11}C_{22} - C_{12}^2},$$

$$H_{25} = \frac{C_{15}C_{12} - C_{16}C_{11}}{C_{11}C_{22} - C_{12}^2}, \quad H_{26} = \frac{C_{16}C_{12} - C_{26}C_{11}}{C_{11}C_{22} - C_{12}^2}$$

(18)

The Airy's stress function $f(x, y, t)$ is defined as

$$N_x = \frac{\partial^2 f}{\partial y^2}, \quad N_y = \frac{\partial^2 f}{\partial x^2}, \quad N_{xy} = -\frac{\partial^2 f}{\partial x \partial y}$$

(19)

Replacing equation (19) into equations (8a) and (8b) yields

$$\frac{\partial^2 u}{\partial t^2} = -\frac{I_1}{J_0}\frac{\partial^2 \varphi_1}{\partial t^2} + \frac{c_1 J_3}{J_0}\frac{\partial^3 w}{\partial x \partial t^2} \tag{20a}$$

$$\frac{\partial^2 v}{\partial t^2} = -\frac{I_1}{J_0}\frac{\partial^2 \varphi_2}{\partial t^2} + \frac{c_1 J_3}{J_0}\frac{\partial^3 w}{\partial y \partial t^2} \tag{20b}$$

Replacing equations (20a) and (20b) into equations (8c) to (8e) leads to

$$
\frac{\partial Q_x}{\partial x} + \frac{\partial Q_y}{\partial y} - c_2\left(\frac{\partial R_x}{\partial x} + \frac{\partial R_y}{\partial y}\right) + N_x\frac{\partial^2 w}{\partial x^2} + 2N_{xy}\frac{\partial^2 w}{\partial x \partial y}
$$
$$
+ N_y\frac{\partial^2 w}{\partial y^2} + c_1\left(\frac{\partial^2 P_x}{\partial x^2} + 2\frac{\partial^2 P_{xy}}{\partial x \partial y} + \frac{\partial^2 P_y}{\partial y^2}\right) - k_1 w + k_2\left(\frac{\partial^2 w}{\partial x^2} + \frac{\partial^2 w}{\partial y^2}\right) + \frac{N_y}{R} + q
$$
$$
= J_0\frac{\partial^2 w}{\partial t^2} + 2\varepsilon J_0\frac{\partial w}{\partial t} + \left(\frac{c_1^2 J_3^2}{J_0} - c_1^2 J_6\right)\left(\frac{\partial^4 w}{\partial x^2 \partial t^2} + \frac{\partial^4 w}{\partial y^2 \partial t^2}\right)
$$
$$
+ \left(I_4 c_1 - \frac{I_1 J_3 c_1}{J_0}\right)\frac{\partial^3 \varphi_1}{\partial x \partial t^2} + \left(I_4 c_1 - \frac{I_1 J_3 c_1}{J_0}\right)\frac{\partial^3 \varphi_2}{\partial y \partial t^2}
\tag{21a}
$$

$$
\frac{\partial M_x}{\partial x} + \frac{\partial M_{xy}}{\partial y} - c_1\left(\frac{\partial P_x}{\partial x} + \frac{\partial P_{xy}}{\partial y}\right) - Q_x + c_2 R_x
$$
$$
= \left(V_2 - \frac{I_1^2}{J_0}\right)\frac{\partial^2 \varphi_1}{\partial t^2} + \left(\frac{c_1 J_3 I_1}{J_0} - c_1 I_4\right)\frac{\partial^3 w}{\partial x \partial t^2}
\tag{21b}
$$

$$
\frac{\partial M_{xy}}{\partial x} + \frac{\partial M_y}{\partial y} - c_1\left(\frac{\partial P_{xy}}{\partial x} + \frac{\partial P_y}{\partial y}\right) - Q_y + c_2 R_y
$$
$$
= \left(V_2 - \frac{I_1^2}{J_0}\right)\frac{\partial^2 \varphi_2}{\partial t^2} + \left(\frac{c_1 J_3 I_1}{J_0} - c_1 I_4\right)\frac{\partial^3 w}{\partial y \partial t^2}
\tag{21c}
$$

By substituting equations (10) and (12) into equation (16) and then into equations (21) gives

$$
R_{11}(w) + R_{12}(\varphi_1) + R_{13}(\varphi_2) + R_{14}(f) + P(x,f) + q = J_0\frac{\partial^2 w}{\partial t^2} + 2\varepsilon J_0\frac{\partial w}{\partial t}
$$
$$
+ \left(\frac{c_1^2 J_3^2}{J_0} - c_1^2 J_6\right)\left(\frac{\partial^4 w}{\partial x^2 \partial t^2} + \frac{\partial^4 w}{\partial y^2 \partial t^2}\right) + \left(I_4 c_1 - \frac{I_1 J_3 c_1}{J_0}\right)\frac{\partial^3 \varphi_1}{\partial x \partial t^2} + \left(I_4 c_1 - \frac{I_1 J_3 c_1}{J_0}\right)\frac{\partial^3 \varphi_2}{\partial y \partial t^2},
$$
$$
R_{21}(w) + R_{22}(\phi_x) + R_{23}(\phi_y) + R_{23}(f) = \left(V_2 - \frac{I_1^2}{J_0}\right)\frac{\partial^2 \varphi_1}{\partial t^2} + \left(\frac{c_1 J_3 I_1}{J_0} - c_1 I_4\right)\frac{\partial^3 w}{\partial x \partial t^2},
$$

$$R_{31}(w) + R_{32}(\phi_x) + R_{33}(\phi_y) + R_{34}(f) = \left(V_2 - \frac{I_1^2}{J_0}\right)\frac{\partial^2\varphi_2}{\partial t^2} + \left(\frac{c_1 J_3 I_1}{J_0} - c_1 I_4\right)\frac{\partial^3 w}{\partial y \partial t^2}$$

(22)

in which

$$R_{11} = \left(G_{11} + c_2 G_{12} - \frac{4G_{12}}{h^2} - \frac{4c_2 G_{32}}{h^2}\right)\frac{\partial^2 w}{\partial x^2} + \left(G_{21} + c_2 G_{22} - \frac{4G_{22}}{h^2} - \frac{4c_2 G_{42}}{h^2}\right)$$
$$\times \frac{\partial^2 w}{\partial y^2} - c_1^2 A_{45}\frac{\partial^4 w}{\partial x^4} - \left(c_1^2 A_{46} + 4c_1^2 A_{63} + c_1^2 A_{55}\right)\frac{\partial^4 w}{\partial x^2 \partial y^2} - c_1^2 A_{56}\frac{\partial^4 w}{\partial y^4},$$

$$R_{12} = \left(G_{11} + c_2 G_{12} - \frac{4G_{12}}{h^2} - \frac{4c_2 G_{32}}{h^2}\right)\frac{\partial\varphi_1}{\partial x} + \left(c_1 A_{43} - c_1^2 A_{45}\right)\frac{\partial^3\varphi_1}{\partial x^3}$$
$$+ \left(2c_1 A_{62} - 2c_1^2 A_{63} + A_{53} c_1 - c_1^2 A_{55}\right)\frac{\partial^3\varphi_1}{\partial x \partial y^2},$$

$$R_{13} = \left(G_{21} + c_2 G_{22} - \frac{4G_{22}}{h^2} - \frac{4c_2 G_{42}}{h^2}\right)\frac{\partial\varphi_2}{\partial y} + \left(A_{54} c_1 - c_1^2 A_{56}\right)\frac{\partial^3\varphi_2}{\partial y^3}$$
$$+ \left(2c_1 A_{62} - 2c_1^2 A_{63} + c_1 A_{44} - c_1^2 A_{46}\right)\frac{\partial^3\varphi_2}{\partial y \partial x^2},$$

$$R_{14} = c_1 A_{42}\frac{\partial^4 f}{\partial x^4} + \left(c_1 A_{41} - 2c_1 A_{61} + A_{52} c_1\right)\frac{\partial^4 f}{\partial x^2 \partial y^2} + A_{51} c_1\frac{\partial^4 f}{\partial y^4} - \frac{1}{R}\frac{\partial^2 f}{\partial y^2},$$

$$P(x,f) = \frac{\partial^2 f}{\partial y^2}\frac{\partial^2 w}{\partial x^2} - 2\frac{\partial^2 f}{\partial x \partial y}\frac{\partial^2 w}{\partial x \partial y} + \frac{\partial^2 f}{\partial y^2}\frac{\partial^2 w}{\partial y^2},$$

$$R_{21} = \left(c_1^2 A_{45} - c_1 A_{15}\right)\frac{\partial^3 w}{\partial x^3} + \left(2c_1^2 A_{63} + c_1^2 A_{46} - c_1 A_{16} - 2c_1 A_{33}\right)\frac{\partial^3 w}{\partial x \partial y^2}$$
$$- \left(G_{11} - c_2^2 G_{32}\right)\frac{\partial w}{\partial x},$$

$$R_{22} = \left(A_{13} - c_1 A_{15} - c_1 A_{43} + c_1^2 A_{45}\right)\frac{\partial^2\phi_x}{\partial x^2}$$
$$+ \left(A_{32} - c_1 A_{33} - c_1 A_{62} + c_1^2 A_{63}\right)\frac{\partial^2\varphi_1}{\partial y^2} - \left(G_{11} - c_2^2 G_{32}\right)\varphi_1,$$

$$R_{23} = \left(A_{14} + A_{32} - c_1 A_{16} - c_1 A_{44} - c_1 A_{33} - c_1 A_{62} + c_1^2 A_{46} + c_1^2 A_{63}\right)\frac{\partial^2\varphi_2}{\partial x \partial y},$$

$$R_{24} = \left(A_{11} - A_{31} - c_1 A_{41} + c_1 A_{61}\right)\frac{\partial^3 f}{\partial x \partial y^2} + \left(A_{12} - c_1 A_{42}\right)\frac{\partial^3 f}{\partial x^3},$$

$$R_{31} = \left(c_1^2 A_{55} + 2c_1^2 A_{63} - 2c_1 A_{33} - c_1 A_{25}\right)\frac{\partial^3 w}{\partial x^2 \partial y}$$
$$+ \left(c_1^2 A_{56} - c_1 A_{26}\right)\frac{\partial^3 w}{\partial y^3} - \left(B_{21} - c_2^2 B_{42}\right)\frac{\partial w}{\partial y},$$

$$R_{32} = \left(A_{32} - c_1 A_{33} + A_{23} - c_1 A_{25} - A_{62}c_1 + c_1^2 A_{63} - A_{53}c_1 + c_1^2 A_{55}\right)\frac{\partial^2 \varphi_1}{\partial x \partial y},$$

$$R_{33} = \left(A_{32} - c_1 A_{33} - A_{62}c_1 + c_1^2 A_{63}\right)\frac{\partial^2 \phi_y}{\partial x^2}$$

$$+ \left(A_{24} - c_1 A_{26} - A_{54}c_1 + c_1^2 A_{56}\right)\frac{\partial^2 \varphi_2}{\partial y^2} - \left(G_{21} - c_2^2 G_{42}\right)\varphi_2, \tag{23}$$

$$R_{34} = \left(A_{22} - A_{31} + A_{61}c_1 - A_{52}c_1\right)\frac{\partial^3 f}{\partial x^2 \partial y} + \left(A_{21} - A_{51}c_1\right)\frac{\partial^3 f}{\partial y^3}$$

Introduction of equations (17) into equation (7), the compatibility equation of the FG-CNTRC cylindrical panel is rewritten as

$$H_{11}\frac{\partial^4 f}{\partial y^4} - H_{22}\frac{\partial^4 f}{\partial x^4} - \left(H_{12} + H_{12} - \frac{1}{C_{31}}\right)\frac{\partial^4 f}{\partial x^2 \partial y^2}$$

$$+ (H_{13} - c_1 H_{15})\frac{\partial^3 \varphi_1}{\partial x \partial y^2} + (H_{23} - c_1 H_{25})\frac{\partial^3 \varphi_1}{\partial x^3} + \left(\frac{C_{32}}{C_{31}} - c_1\frac{C_{33}}{C_{31}}\right)\frac{\partial^3 \varphi_1}{\partial y^2 \partial x}$$

$$+ (H_{14} - c_1 H_{16})\frac{\partial^3 \varphi_2}{\partial y^3} + (H_{24} - c_1 H_{26})\frac{\partial^3 \varphi_2}{\partial x^2 \partial y} + \left(\frac{C_{32}}{C_{31}} - c_1\frac{C_{33}}{C_{31}}\right)\frac{\partial^3 \varphi_2}{\partial x^2 \partial y} \tag{24}$$

$$- c_1 H_{16}\frac{\partial^4 w}{\partial y^4} - c_1 H_{25}\frac{\partial^4 w}{\partial x^4} - \left(c_1 H_{26} + 2c_1\frac{C_{33}}{C_{31}} + c_1 H_{15}\right)\frac{\partial^4 w}{\partial x^2 \partial y^2}$$

$$= \left(\frac{\partial^2 w}{\partial x \partial y}\right)^2 - \frac{\partial^2 w}{\partial x^2}\frac{\partial^2 w}{\partial y^2} + \frac{\partial^2 w}{\partial x^2 R}$$

Solution procedure

In this paper, we assume that four edges of the FG-CNTRC cylindrical panel are immovable and simply supported. The boundary conditions are

$$\begin{aligned} w = u = \varphi_2 = M_x = P_x = 0, \quad N_x = N_{x0} \quad \text{at } x = 0, a, \\ w = v = \varphi_1 = M_y = P_y = 0, \quad N_y = N_{y0} \quad \text{at } y = 0, b \end{aligned} \tag{25}$$

in which N_{x0} and N_{y0} are fictitious compressive edge loads at immovable edges.

The mentioned conditions (25) can be satisfied identically if the approximate solutions are chosen in the following form

$$\begin{bmatrix} w(x,y,t) \\ \varphi_1(x,y,t) \\ \varphi_2(x,y,t) \end{bmatrix} = \begin{bmatrix} W(t)\sin\lambda_m x \sin\delta_n y \\ \Phi_x(t)\cos\lambda_m x \sin\delta_n y \\ \Phi_y(t)\sin\lambda_m x \cos\delta_n y \end{bmatrix} \tag{26}$$

where $\lambda_m = m\pi/a$, $\delta_n = n\pi/b$; m, n are odd natural numbers representing the number of half waves in the x and y directions, respectively; and $W(t)$, Φ_x, Φ_y are the amplitudes of the approximate solutions with condition is dependent on time.

Introduction of equations (26) into the compatibility equation (24), we obtain the stress function f as

$$f(x, y, t) = A_1(t)\cos 2\alpha x + A_2(t)\cos 2\beta y + A_3(t)\sin\alpha x\sin\beta y + \frac{1}{2}N_{x0}y^2 + \frac{1}{2}N_{y0}x^2$$

$$(27)$$

in which

$$A_1 = \frac{W^2\beta^2}{32F_{22}\alpha^2}; \quad A_2 = \frac{W^2\alpha^2}{32F_{11}\beta^2}; \quad A_3 = F_1\Phi_x + F_2\Phi_y - F_3 W \quad (28)$$

and

$$F_1 = \frac{\left[(H_{13} - c_1 H_{15})\alpha\beta^2 + \left(H_{23} - c_1 H_{25} + \dfrac{C_{32}}{C_{31}} - c_1\dfrac{C_{33}}{C_{31}}\right)\alpha^3\right]}{\left[-H_{11}\beta^4 + H_{22}\alpha^4 + \left(2H_{12} - \dfrac{1}{C_{31}}\right)\alpha^2\beta^2\right]}$$

$$F_2 = \frac{\left[(H_{14} - c_1 H_{16})\beta^3 + \left(H_{24} - c_1 H_{26} + \dfrac{C_{32}}{C_{31}} - c_1\dfrac{C_{33}}{C_{31}}\right)\beta\alpha^2\right]}{\left[-H_{11}\beta^4 + H_{22}\alpha^4 + \left(2H_{12} - \dfrac{1}{C_{31}}\right)\alpha^2\beta^2\right]} \quad (29)$$

$$F_3 = \frac{\left[c_1 H_{16}\beta^4 + c_1 H_{25}\alpha^4 + \left(c_1 H_{26} + 2c_1\dfrac{C_{33}}{C_{31}} + c_1 H_{15}\right)\alpha^2\beta^2\right]}{\left[-H_{11}\beta^4 + H_{22}\alpha^4 + \left(2H_{12} - \dfrac{1}{C_{31}}\right)\alpha^2\beta^2\right]}$$

Replacing equations (27) to (29) into equations of motion (24) and then applying Galerkin method yields

$$\left[r_{11} - \left(N_{x0}\alpha^2 + N_{y0}\beta^2\right)\right]W + r_{12}\Phi_x + r_{13}\Phi_y + r_{14}W^2 + r_{15}W^3$$

$$-\frac{1}{R}N_{x0}\frac{16}{\alpha\beta ab} + F_1\beta^2\alpha^2 W\Phi_x\frac{32}{3mn\pi^2} + F_2\beta^2\alpha^2 W\Phi_y\frac{32}{3mn\pi^2} + \frac{16}{mn\pi^2}q$$

$$= 2\varepsilon J_0\frac{\partial W}{\partial t} + n_2\frac{\partial^2 W}{\partial t^2} + \rho_2\alpha\frac{\partial^2\Phi_x}{\partial t^2} + \rho_2\beta\frac{\partial^2\Phi_y}{\partial t^2},$$

$$r_{21}W + r_{22}\Phi_x + r_{23}\Phi_y + r_{24}W^2 = \rho_1\frac{\partial^2\Phi_x}{\partial t^2} + \rho_2\beta\frac{\partial^2 W}{\partial t^2},$$

$$r_{31}W + r_{32}\Phi_x + r_{33}\Phi_y + r_{34}W^2 = \rho_1\frac{\partial^2\Phi_y}{\partial t^2} + \rho_2\beta\frac{\partial^2 W}{\partial t^2} \tag{30}$$

where

$$\rho_1 = V_2 - \frac{I_1^2}{J_0}, \qquad \rho_2 = \frac{c_1 J_3 I_1}{J_0} - c_1 I_4 \tag{31}$$

and specific expressions of coefficients $r_{ij}(i = 1 \div 3, j = 1 \div 3)$, n_1, n_2 are given in Appendix 1.

Consider the FG-CNTRC panel which is subjected temperature environments and simultaneously exposed to uniform external pressure q. The condition on immovability at all edges, i.e., $u = 0$ at $x = 0, a$ and $v = 0$ at $y = 0, b$, is satisfied in an average sense [23,32]

$$\int_0^b \int_0^a \frac{\partial u}{\partial x}dxdy = 0, \qquad \int_0^a \int_0^b \frac{\partial v}{\partial y}dydx = 0 \tag{32}$$

From equations (10) and (17), we obtain the following expressions

$$\begin{aligned}
\frac{\partial u}{\partial x} &= H_{11}\frac{\partial^2 f}{\partial y^2} - H_{12}\frac{\partial^2 f}{\partial x^2} + (H_{13} - c_1 H_{15})\frac{\partial\varphi_1}{\partial x} + (H_{14} - c_1 H_{16})\frac{\partial\varphi_2}{\partial y} \\
&\quad - \frac{1}{2}\left(\frac{\partial w}{\partial x}\right)^2 - c_1 H_{15}\frac{\partial^2 w}{\partial x^2} - c_1 H_{16}\frac{\partial^2 w}{\partial y^2} + H_{11}\Phi_x^1 - H_{12}\Phi_y^1, \\
\frac{\partial v}{\partial y} &= -H_{12}\frac{\partial^2 f}{\partial y^2} + H_{22}\frac{\partial^2 f}{\partial x^2} + (H_{23} - c_1 H_{25})\frac{\partial\varphi_1}{\partial x} + (H_{24} - c_1 H_{26})\frac{\partial\varphi_2}{\partial y} \\
&\quad + \frac{w}{R} - \frac{1}{2}\left(\frac{\partial w}{\partial y}\right)^2 - c_1 H_{25}\frac{\partial^2 w}{\partial x^2} - c_1 H_{26}\frac{\partial^2 w}{\partial y^2} - H_{12}\Phi_x^1 - H_{22}\Phi_y^1
\end{aligned} \tag{33}$$

Putting equations (27)–(29) into equation (33) and then the result into equation (32), we have

$$\begin{aligned}
N_{x0} &= T_{11}W + T_{12}\Phi_x + T_{13}\Phi_y + T_{14}W^2 + T_{15}, \\
N_{y0} &= T_{21}W + T_{22}\Phi_x + T_{23}\Phi_y + T_{24}W^2 + T_{25}
\end{aligned} \tag{34}$$

in which the details of $T_{ij}(i,j = \overline{1,5})$ are found in Appendix 1.

Replacing equations (34) into equation (32) yields

$$S_{11}W + S_{12}\Phi_x + S_{13}\Phi_y + S_{14}W\Phi_x$$

$$+ S_{15} W \Phi_y + S_{16} W^2 + S_{17} W^3 - \frac{T_{15}}{R} \frac{16}{\alpha \beta ab} + \frac{16}{mn\pi^2} q$$

$$= 2\varepsilon J_0 \frac{\partial W}{\partial t} + n_2 \frac{\partial^2 W}{\partial t^2} + \rho_2 \alpha \frac{\partial^2 \Phi_x}{\partial t^2} + \rho_2 \beta \frac{\partial^2 \Phi_y}{\partial t^2},$$

$$r_{21} W + r_{22} \Phi_x + r_{23} \Phi_y + r_{24} W^2 = \rho_1 \frac{\partial^2 \Phi_x}{\partial t^2} + \rho_2 \alpha \frac{\partial^2 W}{\partial t^2},$$

$$r_{31} W + r_{32} \Phi_x + r_{33} \Phi_y + r_{34} W^2 = \rho_1 \frac{\partial^2 \Phi_y}{\partial t^2} + \rho_2 \beta \frac{\partial^2 W}{\partial t^2}$$

(35)

with

$$S_{11} = \left(r_{11} - T_{15}\alpha^2 - \beta^2 T_{25} - \frac{T_{21}}{R} \frac{16}{\alpha \beta ab} \right),$$

$$S_{12} = r_{12} - \frac{T_{12}}{R} \frac{16}{\alpha \beta ab}; \quad S_{13} = r_{13} - \frac{T_{13}}{R} \frac{16}{\alpha \beta ab},$$

$$S_{16} = r_{14} - \left(T_{11}\alpha^2 + T_{21}\beta^2 + \frac{T_{14}}{R} \frac{16}{\alpha \beta ab} \right); \quad S_{17} = r_{15} + \left(\beta^2 T_{24} - T_{14}\alpha^2 \right),$$

$$S_{14} = - \left(T_{12}\alpha^2 + T_{22}\beta^2 + F_1 \beta^2 \alpha^2 \frac{32}{3mn\pi^2} \right); \quad S_{15} = - \left(T_{13}\alpha^2 + T_{23}\beta^2 + F_2 \beta^2 \alpha^2 \frac{32}{3mn\pi^2} \right)$$

(36)

If $q = 0$ and talking linear parts of the set of equation (35), by solving the determinant equation (37), the natural frequencies of the perfect FG-CNTRC cylindrical panel can be determined directly:

$$\begin{vmatrix} S_{11} + n_2 \omega^2 & S_{12} + \rho_2 \frac{m\pi}{a} \omega^2 & S_{13} + \rho_2 \frac{n\pi}{b} \omega^2 \\ r_{21} + \rho_2 \frac{m\pi}{a} \omega^2 & r_{22} + \rho_1 \omega^2 & r_{23} \\ r_{31} + \rho_2 \frac{n\pi}{b} \omega^2 & r_{32} & r_{33} + \rho_1 \omega^2 \end{vmatrix} = 0$$

(37)

By solving equation (37), three values of frequencies of the FG-CNTRC cylindrical panel in the axial, circumferential and radial direction are obtained and the smallest one is considered.

Numerical results and discussion

Validation of the present study

To verify the reliability of the present approach and theory, the natural frequencies $f = \omega/2\pi \, (\text{Hz})$ of Al_2O_3/Ti-$6Al$-$4V$ FGM cylindrical panel in thermal

environments in this paper are compared with results presented by Duc et al. [23] based on the HSDT, which is shown in Table 3. The mechanical properties are chosen as $a/b = 1$, $b/h = 20$. It is clear that a good agreement is obtained in this comparison.

Natural frequency

In this section, we consider influences of many factors which can affect to natural oscillation frequency of the FG-CNTRC cylindrical panels. Specifically, Table 4 shows the effect of types of FG-CNTRC, carbon nanotubes volume fraction V^*_{CNT} and temperature increment ΔT on the natural frequency of FG-CNTRC cylindrical panels with $b/a = 1$, $b/h = 20$, $R/h = 300$. It is easy to see that the value of the natural oscillation frequency of the FG-CNTRC cylindrical panel

Table 3. Comparison of natural frequencies for FGM cylindrical panels $(a = b = 0.1\ m)$.

$(k_1\ (GPa/m),$ $k_2\ (GPa{\cdot}m))$	b/h	$N = 0$		$N = 1$		$N = 5$	
		Present	Duc et al. [23]	Present	Duc et al. [23]	Present	Duc et al. [23]
(0,0)	20	2.815e3	2.971e3	1.654e3	1.722e3	1.422e3	1.465e3
	30	1.926e3	2.001e3	1.056e3	1.161e3	913.4	986.9
	40	1.421e3	1.528e3	816.6	891.7	712.4	753.9
(0.1,0)	20	2.955e3	3.058e3	1.812e3	1.892e3	1.623e3	1.685e3
	30	2.115e3	2.190e3	1.456e3	1.507e3	1.356e3	1.419e3
	40	1.795e3	1.841e3	1.384e3	1.423e3	1.355e3	1.398e3
(0.1,0.02)	20	3.315e3	3.381e3	2.589e3	2.624e3	2.703e3	2.726e3
	30	2.756e3	2.812e3	2.405e3	2.452e3	2.416e3	2.474e3
	40	2.713e3	2.747e3	2.410e3	2.432e3	2.314e3	2.362e3

Table 4. Effect of types of functionally graded carbon nanotubes-reinforced composite, carbon nanotubes volume fraction V^*_{CNT}, and temperature increment ΔT on natural frequencies (s^{-1}) of the functionally graded carbon nanotubes-reinforced cylindrical panel.

$\Delta T\ (K)$	$V^*_{CNT} = 0.12$		$V^*_{CNT} = 0.17$		$V^*_{CNT} = 0.28$	
	FG-A	UD	FG-A	UD	FG-A	UD
0	8976	9171	11541	11730	12487	12640
100	8403	8610	9369	11000	11706	11895
200	7791	8016	8600	10226	9158	11108
400	5250	6675	6807	8472	8989	9344
600	3335	4953	5774	6203	6544	7105

increases when the value of temperature increment is fixed and the value of carbon nanotubes volume fraction increases. In contrast, the value of the natural oscillation frequency of the FG-CNTRC cylindrical panel decreases when the value of temperature increment increases and the value of carbon nanotubes

Table 5. Effects of carbon nanotubes volume fraction, ratio a/h, elastic foundations k_1, k_2, and types of functionally graded carbon nanotubes-reinforced composite on natural frequencies (s^{-1}) of the functionally graded carbon nanotubes-reinforced composite cylindrical panels.

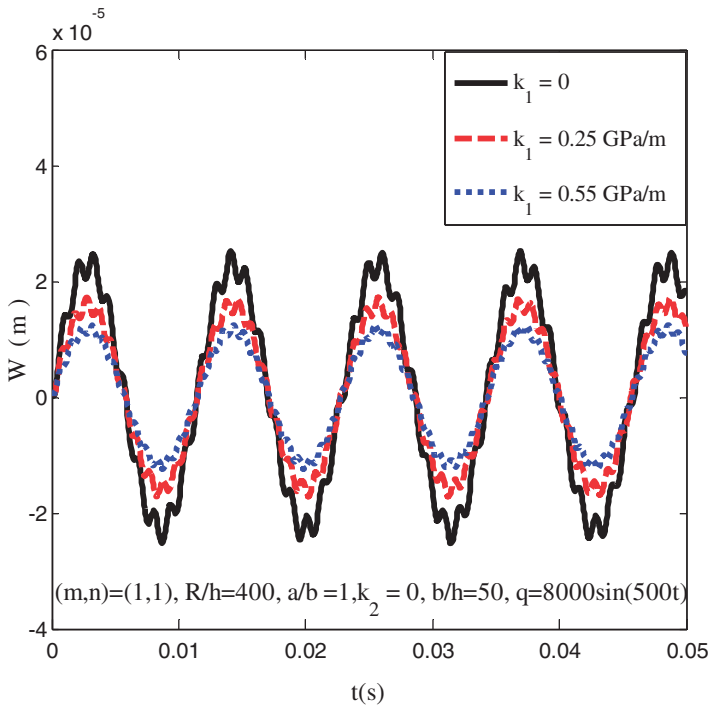| $(k_1 \ (\text{GPa/m}),$ $k_2 \ (\text{GPa·m}))$	a/h	$V^*_{CNT} = 0.12$			$V^*_{CNT} = 0.17$		
		FG-O	FG-A	FG-V	FG-O	FG-A	FG-V
(0,0)	20	1519	1143	704	2822	1744	1277
(0,0)	25	904	817	280	1752	1228	652
(0,0)	30	518	651	252	1131	938	150
(0.1,0.02)	20	2005	640	1489	3110	1151	1833
(0.1,0.02)	25	1457	586	1197	2082	965	1338
(0.1,0.02)	30	1190	456	1062	1545	652	1107

Figure 3. Effects of the Winkler foundation on the nonlinear dynamic response of the functionally graded carbon nanotubes-reinforced composite cylindrical panel.
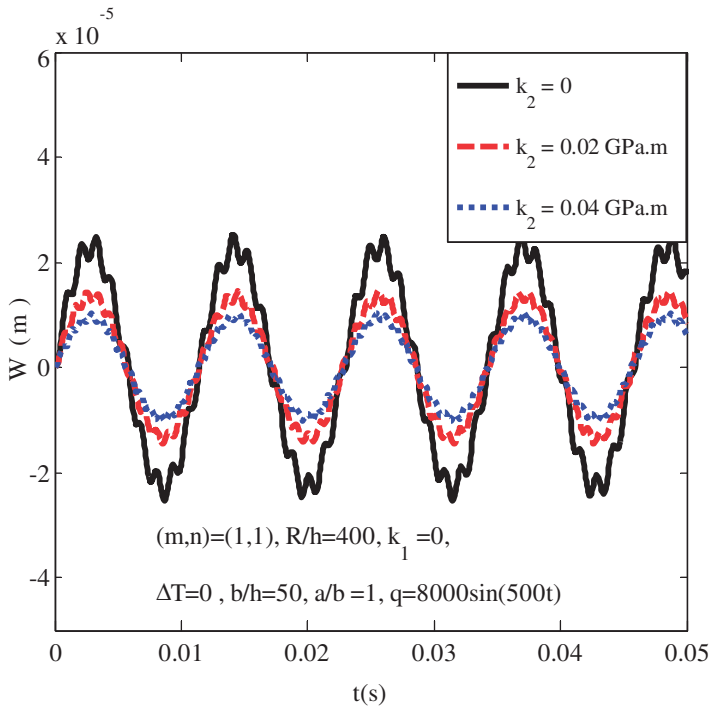
Figure 4. Effects of the Pasternak foundation on the nonlinear dynamic response of the functionally graded carbon nanotubes-reinforced composite cylindrical panel.
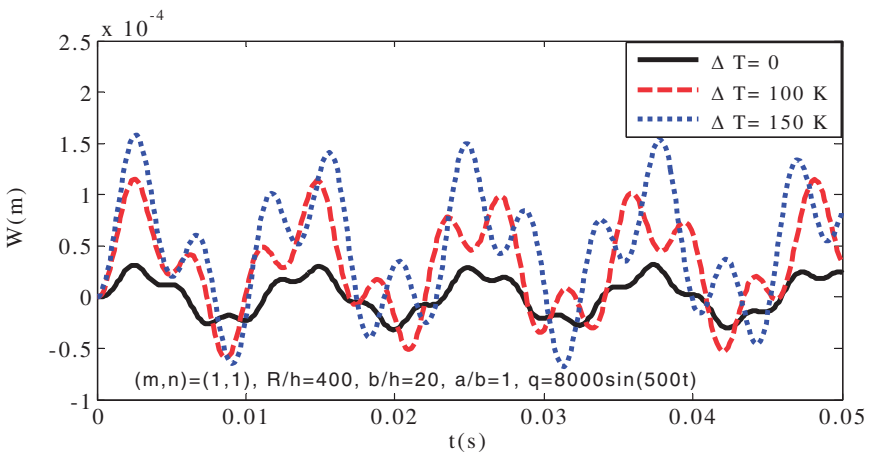

Figure 5. Effects of temperature increment ΔT on the nonlinear dynamic response of the functionally graded carbon nanotubes-reinforced composite cylindrical panel.

volume fraction is fixed. Additionally, this table also highlights that natural oscillation frequency of FG-A cylindrical panel is lower than one of FG-UD cylindrical panel.

Besides, the elastic foundations and geometrical parameter a/h have significant influence on the natural frequencies of the functionally graded carbon nanotubes-reinforced, which is indicated in Table 5. Specifically, the value of the natural frequencies of the functionally graded carbon nanotubes-reinforced cylindrical panel also increases when two parameters of elastic foundations k_1, k_2 or the value of carbon nanotubes volume fraction increases. The change of the value of natural frequency also depends on types of FG-CNTRC. Comparing three types of FG-CNTRC: FG-A, FG-V, and FG-O, the natural frequency of FG-O the highest and the natural frequency of FG-V is the lowest of all. Geometrical parameter is also illustrated in Table 5. It can be seen that the natural frequency of functionally graded carbon nanotubes-reinforced cylindrical panel decreases when the ratio a/h increases.
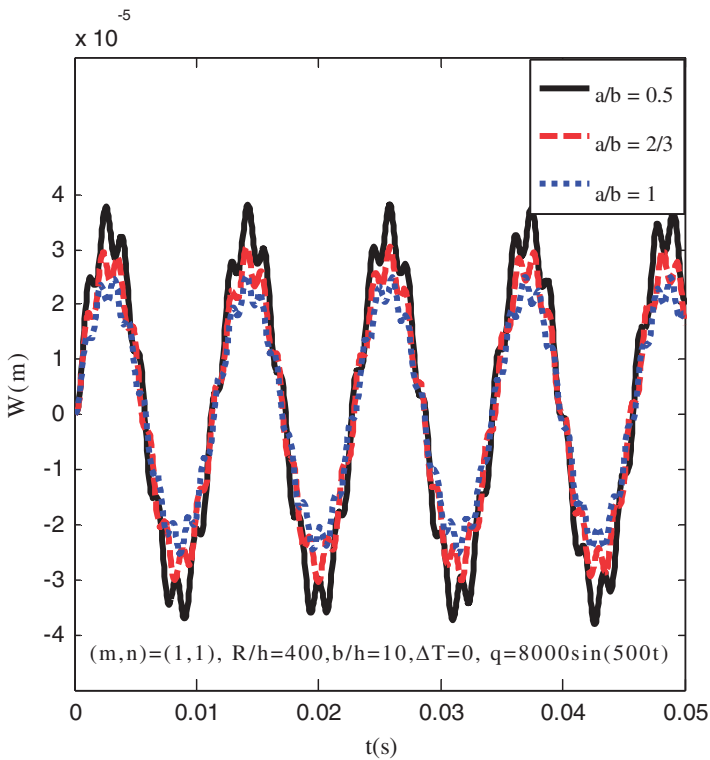

Figure 6. Effects of ratio a/b on the nonlinear dynamic response of the functionally graded carbon nanotubes-reinforced composite cylindrical panel.

Nonlinear dynamic response

Figures 3 and 4 consider the effects of elastic foundations with parameter Pasternak k_1, Winkler k_2 on the nonlinear dynamic response of the FG-CNTRC cylindrical panel in thermal environments with $a/b = 1$, $R/b = 20$. It is clear that the panel fluctuation amplitude decreases when the modulus k_1 and the modulus k_2 increases. On other words, the panel fluctuation amplitude decreases when panel is rested on the elastic foundations. Moreover, from comparison between Figures 3 and 4, we can see that the beneficial effect of the Pasternak foundation with modulus k_1 is better than the effect of Winkler one with modulus k_2.

The influence of temperature increment ΔT on the nonlinear dynamic response of the FG-CNTRC cylindrical panel is shown in Figure 5. When temperature increment ΔT increases, the panel fluctuation amplitude increases.

The effects of geometrical parameters b/a, R/b and b/h on the nonlinear dynamic response of the FG-CNTRC cylindrical panel in thermal environments
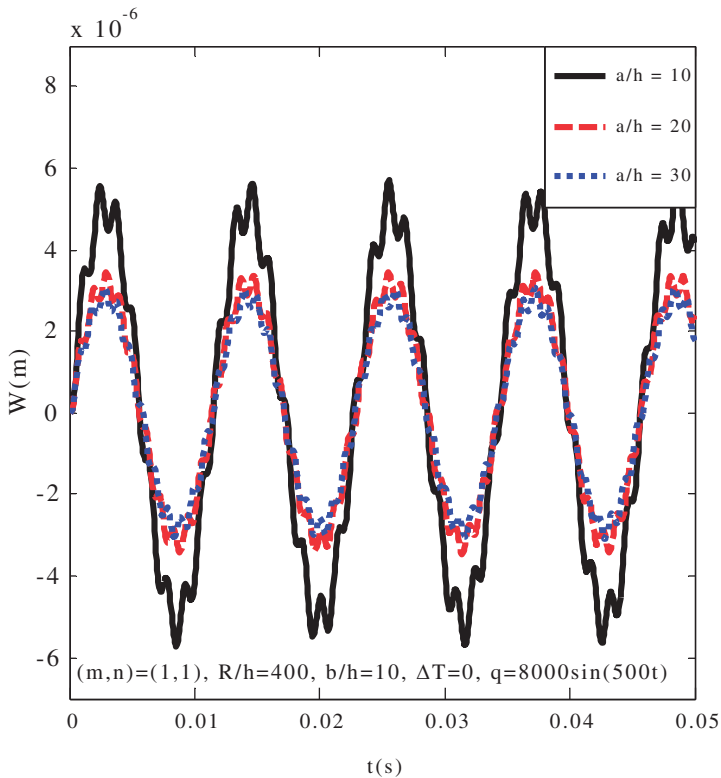

Figure 7. Effects of ratio a/h on the nonlinear dynamic response of the functionally graded carbon nanotubes-reinforced composite cylindrical panel.

are given in Figures 6 to 8, respectively. An increase of the ratio b/a will lead to a decrease of the amplitude of the FG-CNTRC cylindrical panels. The effects of ratios b/h, R/b have similar behaviors.

The comparison panel fluctuation amplitude from the obtained results with different carbon nanotube volume fraction $V_{CNT}^* = 0.12; 0.17; 0.28$ is considered in Figure 9, respectively. We can see that the carbon nanotube volume fraction V_{CNT}^* is chosen as 0.28 the amplitude of FG-CNTRC cylindrical panel is the lowest. And the carbon nanotube volume fraction V_{CNT}^* is chosen 0.12 the amplitude of FG-CNTRC cylindrical panel is the highest. To put it differently, the stiffness of FG-CNTRC cylindrical panel is improved when the FG-CNTRC cylindrical panel is strengthened by the carbon nanotube. It is clear that carbon nanotubes have an important role to increase the stability of functionally graded cylindrical panel.

Figure 10 gives the effect of the type of FG-CNTRC on the nonlinear dynamic response of the FG-CNTRC cylindrical panel in thermal environments. Three types of FG-CNTRC: FG-O, FG-V, and FG-A with geometrical dimensions $a/b = 1$, $b/h = 50$, $R/h = 400$ are considered. Obviously, the amplitude fluctuation of FG-V FG-CNTRC is lower than the amplitude fluctuation of
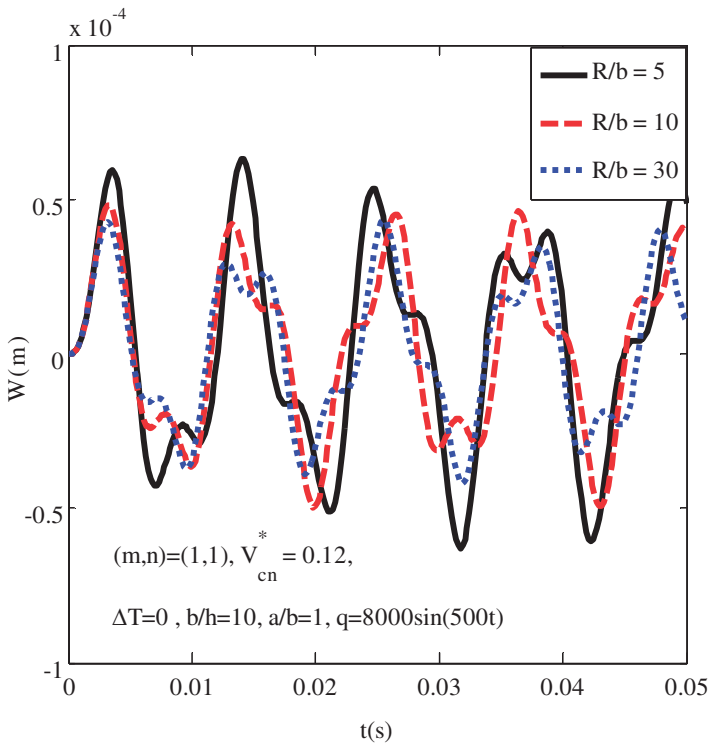

Figure 8. Effects of ratio R/b on the nonlinear dynamic response of the functionally graded carbon nanotubes-reinforced composite cylindrical panel.
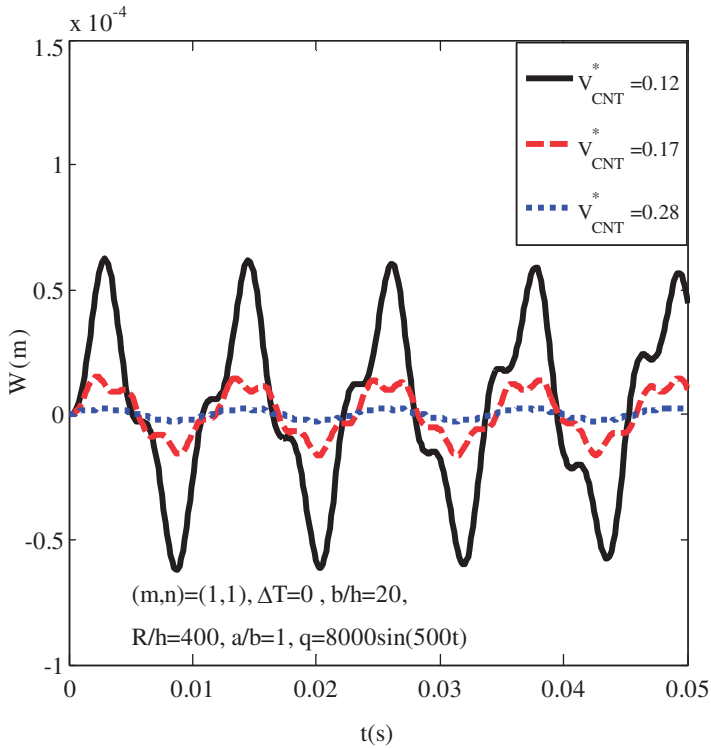
Figure 9. Effects of CNT volume fraction on the nonlinear dynamic response of the functionally graded carbon nanotubes-reinforced composite cylindrical panel.
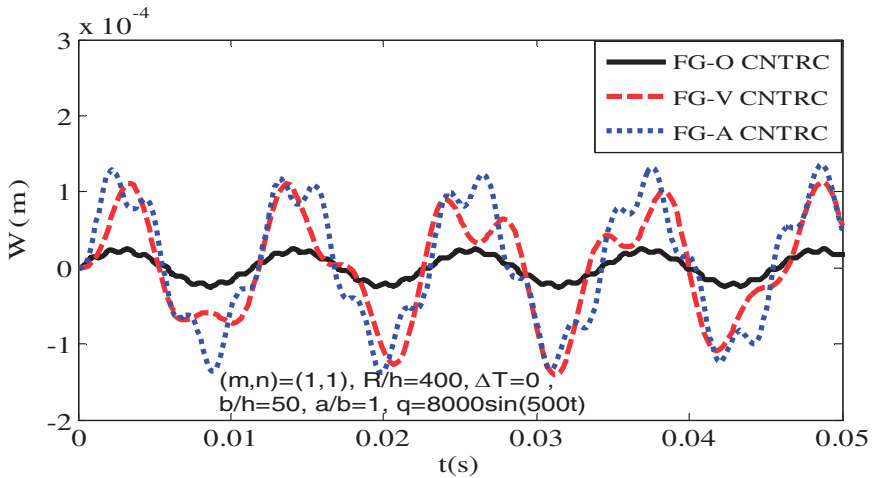

Figure 10. The nonlinear dynamic response of the functionally graded carbon nanotubes-reinforced composite cylindrical panel with different types of carbon nanotubes reinforcements.

FG-AFG-CNTRC and higher than the amplitude fluctuation of FG-O FG-CNTRC. Therefore, FG-O FG-CNTRC should be used when manufactures model.

Conclusions

This work investigated the nonlinear dynamic response and vibration of FG-CNTRC cylindrical panel in thermal environment using both of the HSDT. The panel is supported by elastic foundations and subjected to thermal load. Using stress function, Galerkin method, and fourth-order Runge–Kutta method, the nonlinear dynamic response and natural frequencies of FG-CNTRC cylindrical panels are determined. The reliability of numerical results is evaluated by comparing with other results of the literature. From the obtained results, we can give some conclusions:

1. The stiffness of FG-CNTRC cylindrical panels is improved by carbon nanotube. When the volume fraction of carbon nanotubes increases, the stiffness of panel will increase.
2. The amplitude fluctuation of the FG-CNTRC cylindrical panel strongly changes according to the temperature increment.
3. The beneficial effect of the elastic foundations on the dynamic response of the FG-CNTRC cylindrical panel is clear and the beneficial effect of the Pasternak foundation with modulus k_1 is better than the effect of Winkler one with modulus k_2.
4. The effect of volume fraction of carbon nanotube and type of FG-CNTRC cylindrical panel on the nonlinear dynamic response and natural frequency are considerable. The amplitude fluctuation of FG-V FG-CNTRC is lower than the amplitude fluctuation of FG-A FG-CNTRC and higher than the amplitude fluctuation of FG-O FG-CNTRC.
5. The nonlinear dynamic response of the FG-CNTRC cylindrical panel also is strongly affected by the geometrical parameters.

The advantage of this work is using analytical solution, so the obtained results are expressed explicitly in terms of the input parameters—we may change these parameters and actively control the behaviors of the structures.

Highlights

- Nonlinear dynamic response and vibration
- Functionally graded nanocomposite cylindrical panel reinforced by carbon nanotubes
- The shell resting on elastic foundations in thermal environments
- Based on Reddy's HSDT
- Using analytical solution

ORCID iD

Nguyen Dinh Duc (iD) http://orcid.org/0000-0003-2656-7497

References

1. Shen SH. Thermal buckling and postbuckling behavior of functionally graded carbon nanotube-reinforced composite cylindrical shells. *Compos Part B: Eng* 2012; 43: 1030–1038.
2. Griebel M and Hamaekers J. Molecular dynamics simulations of the elastic moduli of polymer-carbon nanotube composites. *Comput Methods Appl Mech Eng* 2004; 193: 1773–1788.
3. Zhang LW and Liew KM. Postbuckling analysis of axially compressed CNT reinforced functionally graded composite plates resting on Pasternak foundations using an element-free approach. *Compos Struct* 2016; 38: 40–51.
4. Mirzaei M and Kiani Y. Free vibration of functionally graded carbon nanotube reinforced composite cylindrical panels. *Compos Struct* 2016; 142: 45–56.
5. Kolahchi R, Zarei MS, Hajmohammad MH, et al. Wave propagation of embedded viscoelastic FG-CNT-reinforced sandwich plates integrated with sensor and actuator based on refined zigzag theory. *Int J Mech Sci* 2017; 130: 534–545.
6. Zhang LW, Liu WH and Liew KM. Geometrically nonlinear large deformation analysis of triangular CNT-reinforced composite plates. *Int J Non-Linear Mech* 2016; 86: 122–132.
7. Shen SH and Xiang Y. Nonlinear vibration of nanotube-reinforced composite cylindrical panels resting on elastic foundations in thermal environments. *Compos Struct* 2014; 111: 291–300.
8. Shen SH and Xiang Y. Nonlinear bending of nanotube-reinforced composite cylindrical panels resting on elastic foundations in thermal environments. *Eng Struct* 2014; 80: 163–172.
9. Kolahchi R, Safari M and Esmailpour M. Dynamic stability analysis of temperature-dependent functionally graded CNT-reinforced visco-plates resting on orthotropic elastomeric medium. *Compos Struct* 2016; 150: 255–265.
10. Mirzaei M and Kiani Y. Thermal buckling of temperature dependent FG-CNT reinforced composite plates. *Meccanica* 2015; 47: 1–17.
11. Mirzaei M and Kiani Y. Thermal buckling of temperature dependent FG-CNT reinforced composite conical shells. *Aerosp Sci Technol* 2015; 47: 42–53.
12. Shen SH. Postbuckling of nanotube-reinforced composite cylindrical shells in thermal environments. Part II: pressure-loaded shells. *Compos Struct* 2011; 93: 2496–2503.
13. Shen SH. Thermal buckling and postbuckling behavior of functionally graded carbon nanotube-reinforced composite cylindrical shells. *Compos Part B: Eng* 2012; 43: 1030–1038.

14. Bidgoli MR, Karimi MS and Arani AG. Viscous fluid-particle mixture induced vibration and instability of FGCNT-reinforced cylindrical shells integrated with piezoelectric layers. *Steel Compos Struct* 2015; 19: 713–733.

15. Shen HS. Nonliear bending of functionally graded carbon nanotube reinforced composite plate in thermal environments. *Compos Struct* 2009; 91: 3–19.

16. Han Y and Elliott J. Molecular dynamics simulations of the elastic properties of polymer/carbon nanotube composites. *Comput Mater Sci* 2007; 39: 315–323.

17. Hosseini H and Kolahchi R. Seismic response of functionally graded-carbon nanotubes-reinforced submerged viscoelastic cylindrical shell in hygrothermal environment. *Phys E: Low-Dimens Syst Nanostruct* 2018; 102: 101–109.

18. Ovesy HR and Fazilati J. Parametric instability analysis of moderately thick FGM cylindrical panels using FSM. *Compos Struct* 2012; 108–109: 135–143.

19. Viola E, Rossetti L, Fantuzzi N, et al. Static analysis of functionally graded conical shells and panels using the generalized unconstrained third order theory coupled with the stress recovery. *Compos Struct* 2014; 112: 44–65.

20. Thanh NV, Khoa ND, Tuan ND, et al. Nonlinear dynamic response and vibration of functionally graded carbon nanotubes reinforced composite (FG-CNTRC) shear deformable plates with temperature dependence material properties and surrounded on elastic foundations. *J Therm Stress* 2017; 40: 1254–1274.

21. Ou X, Yao X, Zhang R, et al. Nonlinear dynamic response analysis of cylindrical composite stiffened laminates based on the weak form quadrature element method. *Compos Struct* 2018; 203: 446–457.

22. Duc ND and Quan TQ. Nonlinear response of imperfect eccentrically stiffened FGM cylindrical panels on elastic foundation subjected to mechanical loads. *Eur J Mech A Solids* 2014; 46: 60–71.

23. Duc ND, Tuan ND, Quan TQ, Quyen NV, Anh TV. Nonlinear mechanical, thermal and thermo-mechanical postbuckling of imperfect eccentrically stiffened thin FGM cylindrical panels on elastic foundations. *J Sandw Struct Mater* 2015; 96: 155–168.

24. Thu PV and Duc ND. Nonlinear stability analysis of imperfect three-phase sandwich laminated polymer nanocomposite panels resting on elastic foundations in thermal environments. *VNU J Sci Math Phys* 2016; 32: 20–36.

25. Shen SH and Wang H. Nonlinear bending of FGM cylindrical panels resting on elastic foundations in thermal environments. *Eur J Mech A Solids* 2015; 49: 49–59.

26. Kiani Y, Sadighi M and Eslami MR. Dynamic analysis and active control of smart doubly curved FGM panels. *Compos Struct* 2013; 102: 205–216.

27. Duc ND, Seung-Eock K, Quan TQ, et al. Nonlinear dynamic response and vibration of nanocomposite multilayer organic solar cell. *Compos Struct* 2018; 184: 1137–1144.

28. Cong PH, Anh VM and Duc ND. Nonlinear dynamic response of eccentrically stiffened FGM plate using Reddy's TSDT in thermal environment. *J Therm Stress* 2017; 40: 704–732.

29. Najafi F, Shojaeefard MH and Googarchin HS. Nonlinear dynamic response of FGM beams with Winkler–Pasternak foundation subject to noncentral low velocity impact in thermal field. *Compos Struct* 2017; 167: 132–143.

30. Duc ND. Nonlinear thermal dynamic analysis of eccentrically stiffened S-FGM circular cylindrical shells surrounded on elastic foundations using the Reddy's third-order shear deformation shell theory. *Eur J Mech A Solids* 2016; 58: 10–30.

31. Panday S and Pradyumna S. A finite element formulation for thermally induced vibrations of functionally graded material sandwich plates and shell panels. *Compos Struct* 2017; 160: 877–886.

32. Duc ND and Quan TQ. Transient responses of functionally graded double curved shallow shells with temperature-dependent material properties in thermal environment. *Eur J Mech A Solids* 2014; 47: 101–123.

33. Yang J and Shen SH. Vibration characteristics and transient response of shear-deformable functionally graded plates in thermal environments. *J Sound Vib* 2002; 255: 579–602.

34. Duc ND, Cong PH, Tuan ND, et al. Nonlinear vibration and dynamic response of imperfect eccentrically stiffened shear deformable sandwich plate with functionally graded material in thermal environment. *J Sandw Struct Mater* 2016; 18: 445–473.

35. Yang J, Liew KM, Wu YF, et al. Thermo-mechanical post-buckling of FGM cylindrical panels with temperature-dependent properties. *Int J Solids Struct* 2006; 43: 307–324.

36. Matsumaga H. Free vibration and stability of functionally graded shallow shells according to a 2-D higher-order deformation theory. *Compos Struct* 2008; 84: 132–146.

37. Duc ND. *Nonlinear static and dynamic stability of functionally graded plates and shells.* Hanoi: Vietnam National University Press, 2014.

38. Brush DD and Almroth BO. *Buckling of bars, plates and shells.* New York: McGraw-Hill, 1975.

39. Reddy JN. *Mechanics of laminated composite plates and shells: theory and analysis.* Boca Raton: CRC Press, 2004.

Appendix 1

$$G_{11} = \sum_{k=0}^{N} Q_{44}(h_k - h_{k-1}), \quad G_{12} = \sum_{k=0}^{N} Q_{44} \frac{h_k^3 - h_{k-1}^3}{3},$$

$$G_{21} = \sum_{k=0}^{N} Q_{55}(h_k - h_{k-1}), \quad G_{22} = \sum_{k=0}^{N} Q_{55} \frac{h_k^3 - h_{k-1}^3}{3},$$

$$G_{32} = \sum_{k=0}^{N} Q_{44} \frac{h_k^5 - h_{k-1}^5}{5}, \quad G_{42} = \sum_{k=0}^{N} Q_{55} \frac{h_k^5 - h_{k-1}^5}{5},$$

$$C_{75} = \sum_{k=0}^{N} Q_{11} \frac{h_k^7 - h_{k-1}^7}{7}, \quad C_{76} = \sum_{k=0}^{N} Q_{12} \frac{h_k^7 - h_{k-1}^7}{7},$$

$$C_{86} = \sum_{k=0}^{N} Q_{22} \frac{h_k^7 - h_{k-1}^7}{7}, \quad C_{93} = \sum_{k=0}^{N} Q_{66} \frac{h_k^7 - h_{k-1}^7}{7},$$

$$C_{11} = \sum_{k=0}^{N} Q_{11}(h_k - h_{k-1}), \quad C_{12} = \sum_{k=0}^{N} Q_{12}(h_k - h_{k-1}),$$

$$C_{13} = \sum_{k=0}^{N} Q_{11} \frac{(h_k - h_{k-1})^2}{2}, \quad C_{14} = \sum_{k=0}^{N} Q_{12} \frac{h_k^2 - h_{k-1}^2}{2},$$

$$C_{15} = \sum_{k=0}^{N} Q_{11} \frac{h_k^4 - h_{k-1}^4}{4}, \quad C_{16} = \sum_{k=0}^{N} Q_{12} \frac{h_k^4 - h_{k-1}^4}{4},$$

$$C_{22} = \sum_{k=0}^{N} Q_{22}(h_k - h_{k-1}), \quad C_{24} = \sum_{k=0}^{N} Q_{22} \frac{h_k^2 - h_{k-1}^2}{2},$$

$$C_{43} = \sum_{k=0}^{N} Q_{11} \frac{h_k^3 - h_{k-1}^3}{3}, \quad C_{44} = \sum_{k=0}^{N} Q_{12} \frac{h_k^3 - h_{k-1}^3}{3},$$

$$C_{45} = \sum_{k=0}^{N} Q_{11} \frac{h_k^5 - h_{k-1}^5}{5}, \quad C_{46} = \sum_{k=0}^{N} Q_{12} \frac{h_k^5 - h_{k-1}^5}{5},$$

$$C_{26} = \sum_{k=0}^{N} Q_{22} \frac{h_k^4 - h_{k-1}^4}{4}, \quad C_{31} = \sum_{k=0}^{N} Q_{66}(h_k - h_{k-1}),$$

$$C_{32} = \sum_{k=0}^{N} Q_{66} \frac{h_k^2 - h_{k-1}^2}{2}, \quad C_{33} = \sum_{k=0}^{N} Q_{66} \frac{h_k^4 - h_{k-1}^4}{4},$$

$$C_{54} = \sum_{k=0}^{N} Q_{22} \frac{h_k^3 - h_{k-1}^3}{3}, \quad C_{56} = \sum_{k=0}^{N} Q_{22} \frac{h_k^5 - h_{k-1}^5}{5},$$

$$C_{62} = \sum_{k=0}^{N} Q_{66} \frac{h_k^3 - h_{k-1}^3}{3}, \quad C_{63} = \sum_{k=0}^{N} Q_{66} \frac{h_k^5 - h_{k-1}^5}{5},$$

$$\Phi_x^1 = \sum_{k=0}^{N} \int_{h_{k-1}}^{h_k} Q_{11}\alpha_{11}z\Delta T \mathrm{d}z + \sum_{k=0}^{N} \int_{h_{k-1}}^{h_k} Q_{12}\alpha_{22}z\Delta T \mathrm{d}z,$$

$$\Phi_x^3 = \sum_{k=0}^{N} \int_{h_{k-1}}^{h_k} Q_{11}\alpha_{11}z^2\Delta T \mathrm{d}z + \sum_{k=0}^{N} \int_{h_{k-1}}^{h_k} Q_{12}\alpha_{22}z^2\Delta T \mathrm{d}z,$$

$$\Phi_x^5 = \sum_{k=0}^{N} \int_{h_{k-1}}^{h_k} Q_{11}\alpha_{11}z^3\Delta T \mathrm{d}z + \sum_{k=0}^{N} \int_{h_{k-1}}^{h_k} Q_{12}\alpha_{22}z^3\Delta T \mathrm{d}z,$$

$$\Phi_y^1 = \sum_{k=0}^{N} \int_{h_{k-1}}^{h_k} Q_{12}\alpha_{11}z\Delta T \mathrm{d}z + \sum_{k=0}^{N} \int_{h_{k-1}}^{h_k} Q_{22}\alpha_{22}z\Delta T \mathrm{d}z,$$

$$\Phi_y^3 = \sum_{k=0}^{N} \int_{h_{k-1}}^{h_k} Q_{12}\alpha_{11}z^2\Delta T \mathrm{d}z + \sum_{k=0}^{N} \int_{h_{k-1}}^{h_k} Q_{22}\alpha_{22}z^2\Delta T \mathrm{d}z,$$

$$\Phi_y^5 = \sum_{k=0}^{N} \int_{h_{k-1}}^{h_k} Q_{12}\alpha_{11}z^3\Delta T \mathrm{d}z + \sum_{k=0}^{N} \int_{h_{k-1}}^{h_k} Q_{22}\alpha_{22}z^3\Delta T \mathrm{d}z,$$

$$A_{11} = C_{13}H_{11} - C_{14}H_{12}, \quad A_{12} = C_{13}H_{12} + C_{14}H_{22}, \quad A_{13} = C_{13}H_{13} + C_{14}H_{23} + C_{43},$$
$$A_{14} = C_{13}H_{14} + C_{14}H_{24} + C_{44}, \quad A_{15} = C_{13}H_{15} + C_{14}H_{25} + C_{45},$$
$$A_{16} = C_{13}H_{16} + C_{14}H_{26} + C_{46},$$
$$A_{17} = C_{13}H_{11} - C_{14}H_{12}, \quad A_{18} = C_{13}H_{12} + C_{14}H_{22}, \quad A_{21} = C_{14}H_{11} - C_{24}H_{12},$$
$$A_{22} = C_{14}H_{12} + C_{24}H_{22}, \quad A_{23} = C_{14}H_{13} + C_{24}H_{23} + C_{44},$$
$$A_{24} = C_{14}H_{14} + C_{24}H_{24} + C_{54},$$
$$A_{25} = C_{14}H_{15} + C_{24}H_{25} + C_{46}, \quad A_{26} = C_{14}F_{16} + C_{24}F_{26} + C_{56},$$
$$A_{27} = C_{14}H_{11} - C_{24}H_{12},$$
$$A_{28} = C_{14}H_{12} + C_{24}H_{22}, \quad A_{31} = \frac{C_{32}}{C_{31}}, \quad A_{32} = \left(C_{62} - \frac{C_{32}^2}{C_{31}}\right),$$
$$A_{33} = \left(C_{63} - \frac{C_{33}C_{32}}{C_{31}}\right),$$

$$A_{41} = C_{15}H_{11} - C_{16}H_{12}, \quad A_{42} = C_{15}H_{12} + C_{16}H_{22}, \quad A_{43} = C_{15}H_{13} + C_{16}H_{23} + C_{45},$$
$$A_{44} = C_{15}H_{14} + C_{16}H_{24} + C_{46}, \quad A_{45} = C_{15}H_{15} + C_{16}H_{25} + C_{75},$$
$$A_{46} = C_{15}H_{16} + C_{16}H_{26} + C_{76},$$
$$A_{47} = C_{15}H_{11} - C_{16}H_{12}, \quad A_{48} = C_{15}H_{12} + C_{16}H_{22}, \quad A_{51} = C_{16}H_{11} - C_{26}H_{12},$$
$$A_{52} = C_{16}H_{12} + C_{26}H_{22}, \quad A_{53} = C_{16}H_{13} + C_{26}H_{23} + A_{46},$$
$$A_{54} = C_{16}H_{14} + C_{26}H_{24} + C_{56},$$
$$A_{55} = C_{16}H_{15} + C_{26}H_{25} + C_{76}, \quad A_{56} = C_{16}H_{16} + C_{26}H_{26} + C_{86},$$
$$A_{57} = C_{16}H_{11} - C_{26}H_{12},$$
$$A_{58} = C_{16}H_{12} + C_{26}H_{22}, \quad A_{61} = \frac{C_{33}}{C_{31}}, \quad A_{62} = \left(C_{63} - \frac{C_{32}C_{33}}{C_{31}}\right),$$
$$A_{63} = \left(C_{93} - \frac{C_{33}^2}{C_{31}}\right),$$

$$r_{11} = -\left(G_{11} + c_2 G_{12} - \frac{4G_{12}}{h^2} - \frac{4c_2 G_{32}}{h^2}\right)\alpha^2 W - \left(G_{21} + c_2 G_{22} - \frac{4G_{22}}{h^2} - \frac{4c_2 G_{42}}{h^2}\right)\beta^2 W$$
$$- c_1^2 A_{45}\alpha^4 - \left(c_1^2 A_{46} + 4c_1^2 A_{63} + c_1^2 A_{55}\right)\alpha^2\beta^2 - c_1^2 A_{56}\beta^4 W - k_1 - k_2\left(\alpha^2 + \beta^2\right)$$
$$- c_1 A_{42}\alpha^4 H_3 - \left(c_1 A_{41} - 2c_1 A_{61} + A_{52}c_1\right)F_3\alpha^2\beta^2 - \beta^4 F_3 - \frac{1}{R}F_3\alpha^2,$$
$$r_{12} = -\left(G_{11} + c_2 G_{12} - \frac{4G_{12}}{h^2} - \frac{4c_2 G_{32}}{h^2}\right)\alpha + \left(c_1 A_{43} - c_1^2 A_{45}\right)\alpha^3$$
$$+ \left(2c_1 A_{62} - 2c_1^2 A_{63} + A_{53}c_1 - c_1^2 A_{55}\right)\alpha\beta^2 + c_1 A_{42}\alpha^4 H_1$$
$$+ \left(c_1 A_{41} - 2c_1 A_{61} + A_{52}c_1\right)F_1\alpha^2\beta^2 + \beta^4 F_1 + \frac{\alpha^2}{R}F_1\Phi,$$

$$r_{13} = -\left(G_{21} + c_2 G_{22} - \frac{4G_{22}}{h^2} - \frac{4c_2 G_{42}}{h^2}\right)\beta + \left(A_{54}c_1 - c_1^2 A_{56}\right)\beta^3$$
$$+ \left(2c_1 A_{62} - 2c_1^2 A_{63} + c_1 A_{44} - c_1^2 A_{46}\right)\alpha^2\beta$$
$$+ c_1 A_{42}\alpha^4 F_2 + (c_1 A_{41} - 2c_1 A_{61} + A_{52}c_1)\alpha^2\beta^2 F_2 + \beta^4 F_2 + \frac{\alpha^2}{R}F_2,$$

$$r_{14} = c_1 A_{42}\frac{\beta^2}{4H_{22}}\alpha^2 + A_{51}c_1\frac{\alpha^2\beta^2}{4H_{11}} - \frac{1}{R}\frac{2\alpha^2 a^2 b^2}{3H_{11}mn\pi^2} - -F_3\beta^2\alpha^2\frac{32}{3mn\pi^2},$$

$$r_{15} = -2\frac{\alpha^4}{32H_{11}} - 2\frac{\beta^4}{32H_{22}},$$

$$r_{23} = -\left(A_{14} + A_{32} - c_1 A_{16} - c_1 A_{44} - c_1 A_{33} - c_1 A_{62} + c_1^2 A_{46} + c_1^2 A_{63}\right)\alpha\beta$$
$$- \left[(A_{11} - A_{31} - c_1 A_{41} + c_1 A_{61})\beta^2\alpha + (A_{12} - c_1 A_{42})\alpha^3\right]F_2,$$

$$r_{24} = (A_{12} - c_1 A_{42})\frac{8\beta}{3H_{22}ab},$$

$$r_{31} = -\left(c_1^2 A_{55} + 2c_1^2 A_{63} - 2c_1 A_{33} - c_1 A_{25}\right)\alpha^2\beta$$
$$- \left(c_1^2 A_{56} - c_1 A_{26}\right)\beta^3 - \left(G_{21} - c_2^2 G_{42}\right)\beta$$
$$+ \left[(A_{22} - A_{31} + A_{61}c_1 - A_{52}c_1)\alpha^2\beta + \beta^3(A_{21} - A_{51}c_1)\right]F_3,$$

$$r_{21} = -\left(c_1^2 A_{45} - c_1 A_{15}\right)\alpha^3 - \left(G_{11} - c_2^2 G_{32}\right)\alpha - \left(2c_1^2 A_{63} + c_1^2 A_{46} - c_1 A_{16} - 2c_1 A_{33}\right)\alpha\beta^2$$
$$+ \left[(A_{11} - A_{31} - c_1 A_{41} + c_1 A_{61})\beta^2\alpha + (A_{12} - c_1 A_{42})\alpha^3\right]H_3,$$

$$r_{22} = -\left(A_{13} - c_1 A_{15} - c_1 A_{43} + c_1^2 A_{45}\right)\alpha^2 - \left(A_{32} - c_1 A_{33} - c_1 A_{62} + c_1^2 A_{63}\right)\beta^2$$
$$- \left(G_{11} - c_2^2 G_{32}\right)\Phi_x - \left[(A_{11} - A_{31} - c_1 A_{41} + c_1 A_{61})\beta^2\alpha + (A_{12} - c_1 A_{42})\alpha^3\right]F_1,$$

$$r_{32} = -\left(A_{32} - c_1 A_{33} + A_{23} - c_1 A_{25} - A_{62}c_1 + c_1^2 A_{63} - A_{53}c_1 + c_1^2 A_{55}\right)\alpha\beta$$
$$- \left[(A_{22} - A_{31} + A_{61}c_1 - A_{52}c_1)\alpha^2\beta + \beta^3(A_{21} - A_{51}c_1)\right]F_1,$$

$$r_{33} = -\left(A_{32} - c_1 A_{33} - A_{62}c_1 + c_1^2 A_{63}\right)\alpha^2\Phi_y - \left(A_{24} - c_1 A_{26} - A_{54}c_1 + c_1^2 A_{56}\right)\beta^2$$
$$- \left(G_{21} - c_2^2 G_{42}\right)\Phi_y - \left[(A_{22} - A_{31} + A_{61}c_1 - A_{52}c_1)\alpha^2\beta + \beta^3(A_{21} - A_{51}c_1)\right]H_2,$$

$$r_{34} = (A_{21} - A_{51}c_1)\frac{\alpha}{H_{11}}\frac{8}{3ab},$$

$$n_1 = -\frac{E_1}{16}\left(\left(\frac{m\pi}{a}\right)^4 + \left(\frac{n\pi}{b}\right)^4\right),$$

$$n_2 = J_0 + c_1^2\left(J_6 - \frac{J_3^2}{J_0}\right)\left(\left(\frac{m\pi}{a}\right)^2 + \left(\frac{n\pi}{b}\right)^2\right),$$

$$T_{11} = -F_3\beta \frac{4}{\alpha ab} W - \frac{\left[H_{12}\left(c_1 H_{25}\alpha^2 + c_1 H_{26}\beta^2 + \frac{1}{R}\right) + H_{22}\left(c_1 H_{15}\alpha^2 + c_1 H_{16}\beta^2\right)\right]}{H_{11}H_{22} - H_{12}^2} \frac{4}{\alpha\beta ab},$$

$$T_{12} = F_1\beta \frac{4}{\alpha ab}\Phi_x - \frac{[H_{12}[-F_1 H_{22}\alpha + (c_1 H_{25} - H_{23})] + H_{22}[F_1 H_{12}\alpha + (c_1 H_{15} - H_{13})]]}{H_{11}H_{22} - H_{12}^2}\frac{4}{\beta ab},$$

$$T_{13} = \frac{[H_{22}[F_2 H_{11}\beta - (c_1 H_{16} - H_{14})] - H_{12}[F_2 H_{12}\beta + (c_1 H_{26} - H_{24})]]}{H_{11}H_{22} - H_{12}^2}\frac{4}{\alpha ab},$$

$$T_{14} = \left(\frac{H_{22}\alpha^2}{8} + \frac{H_{12}\beta^2}{8}\right)\frac{1}{H_{11}H_{22} - H_{12}^2}; \quad S_{15} = -\frac{H_{22}}{H_{11}H_{22} - H_{12}^2}\left(H_{11}\Phi_x^1 - H_{12}\Phi_y^1\right)$$

$$- \frac{H_{12}}{H_{11}H_{22} - H_{12}^2}\left(-H_{12}\Phi_x^1 - H_{22}\Phi_y^1\right),$$

$$T_{21} = -F_3\alpha \frac{4}{\beta ab} W - \frac{\left[H_{12}\left(c_1 H_{15}\alpha^2 + c_1 H_{16}\beta^2\right) + H_{11}\left(c_1 H_{25}\alpha^2 + c_1 H_{26}\beta^2 + \frac{1}{R}\right)\right]}{H_{11}H_{22} - H_{12}^2}\frac{4}{\alpha\beta ab},$$

$$T_{22} = -\frac{[H_{12}[F_1 H_{12}\alpha + (c_1 H_{15} - H_{13})] + H_{11}[-F_1 H_{22}\alpha + (c_1 H_{25} - H_{23})]]}{H_{11}H_{22} - H_{12}^2}\Phi_x \frac{4}{\beta ab},$$

$$T_{23} = F_2\alpha \frac{4}{\beta ab} + \frac{[H_{12}[F_2 H_{11}\beta - (c_1 H_{16} - H_{14})] - H_{11}[F_2 H_{12}\beta + (c_1 H_{26} - H_{24})]]}{H_{11}H_{22} - H_{12}^2}\frac{4}{\alpha ab},$$

$$T_{24} = \frac{\left(H_{12}\alpha^2 + H_{11}\beta^2\right)}{8\left(H_{11}H_{22} - H_{12}^2\right)}; \quad T_{25} = -\frac{H_{12}}{H_{11}H_{22} - H_{12}^2}\left(H_{11}\Phi_x^1 - H_{12}\Phi_y^1\right)$$

$$- \frac{H_{11}}{H_{11}H_{22} - H_{12}^2}\left(-H_{12}\Phi_x^1 + H_{22}\Phi_y^1\right).$$